

Neutral and Cationic Zirconium Benzyl Complexes Containing Bidentate Pyridine–Alkoxide Ligands. Synthesis and Olefin Polymerization Chemistry of $(\text{pyCR}_2\text{O})_2\text{Zr}(\text{CH}_2\text{Ph})_2$ and $(\text{pyCR}_2\text{O})_2\text{Zr}(\text{CH}_2\text{Ph})^+$ Complexes

Toru Tsukahara, Dale C. Swenson, and Richard F. Jordan*

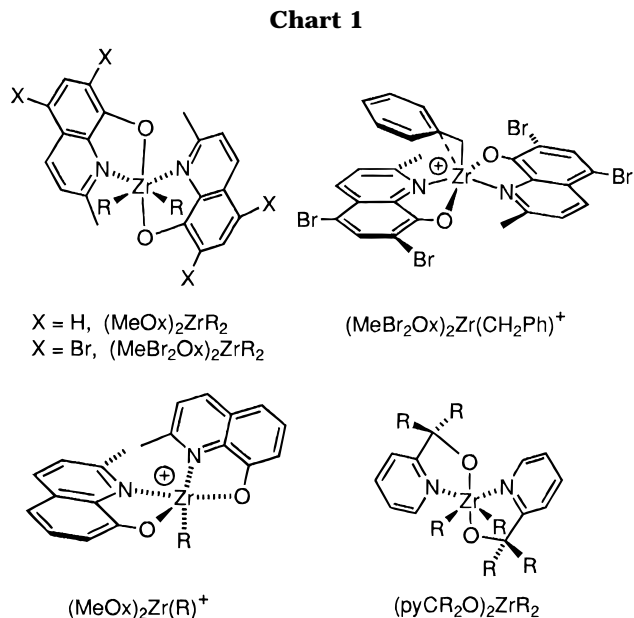
Department of Chemistry, University of Iowa, Iowa City, Iowa 52242

Received March 24, 1997[®]

The reaction of $\text{Zr}(\text{CH}_2\text{Ph})_4$ with the pyridine alcohols 6-py $\text{CR}^1\text{R}^2\text{OH}$ (**2a**, $\text{R}^1 = \text{R}^2 = \text{CF}_3$; **2b**, $\text{R}^1 = \text{R}^2 = \text{Me}$; **2c**, $\text{R}^1 = \text{H}$, $\text{R}^2 = \text{CF}_3$) yields dibenzyl complexes $(\text{pyCR}^1\text{R}^2\text{O})_2\text{Zr}(\text{CH}_2\text{Ph})_2$ (**3a–c**). These species adopt distorted octahedral structures with a *trans*-O, *cis*-N, *cis*-C ligand arrangement but undergo rapid inversion of configuration at Zr on the NMR time scale, with racemization barriers in the range from 8.6 (**3b**) to 10.1 (**3c**) kcal/mol. **3a** and **3b** react with $\text{B}(\text{C}_6\text{F}_5)_3$ to yield $[(\text{pyCR}^1\text{R}^2\text{O})_2\text{Zr}(\text{CH}_2\text{Ph})][\text{PhCH}_2\text{B}(\text{C}_6\text{F}_5)_3]$ (**6a,b**) and with $[\text{HNMe}_2\text{Ph}][\text{B}(\text{C}_6\text{F}_5)_4]$ to yield $[(\text{pyCR}^1\text{R}^2\text{O})_2\text{Zr}(\text{CH}_2\text{Ph})][\text{B}(\text{C}_6\text{F}_5)_4]$ (**7a,b**). NMR spectra indicate that **6a,b** and **7a,b** are not strongly ion-paired in CD_2Cl_2 . **6a** polymerizes ethylene and 1-hexene to low molecular weight polymers. $[(\text{pyCH}(\text{CF}_3)\text{O})_2\text{Zr}(\text{CH}_2\text{Ph})][\text{PhCH}_2\text{B}(\text{C}_6\text{F}_5)_3]$ (**6c**, generated *in situ*) is much less active for ethylene polymerization than **6a**, and **6b** is inactive.

Introduction

We recently described the synthesis of a series of zirconium alkyl complexes of the general type $(\text{Ox})_2\text{ZrR}_2$ which contain methyl- and bromo-substituted quinolinolato (Ox^-) ancillary ligands (Chart 1).¹ These species adopt chiral C_2 -symmetric structures with a *trans*-O, *cis*-N, *cis*-R ligand arrangement but undergo inversion of configuration at the metal (Λ/Δ interconversion, i.e., racemization) on the NMR time scale at elevated temperatures. Protonolysis of $(\text{Ox})_2\text{ZrR}_2$ with HNR_3^+ reagents yields base-free $(\text{Ox})_2\text{ZrR}^+$ cations, which are of interest because of their relationship to $\text{Cp}_2\text{Zr}(\text{R})^+$ cations, the active species in metallocene-based olefin polymerization catalysts.² The structures and reactivity of $(\text{Ox})_2\text{Zr}(\text{CH}_2\text{Ph})^+$ species are quite sensitive to the quinolinolato ligand donor properties. $(\text{MeBr}_2\text{Ox})_2\text{Zr}(\eta^2\text{-CH}_2\text{Ph})^+$ adopts a distorted square pyramidal structure with an η^2 -benzyl group in the apical position and a *trans*-O, *trans*-N arrangement of basal ligands and is an active ethylene polymerization catalyst. In contrast,



[®] Abstract published in *Advance ACS Abstracts*, June 15, 1997.

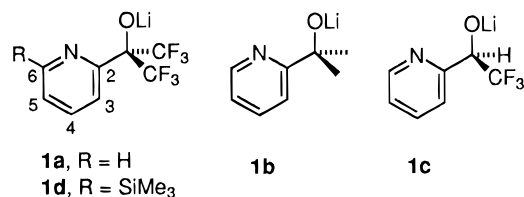
(1) Bei, X.; Swenson, D. C.; Jordan, R. F. *Organometallics* **1997**, *16*, 3282.

(2) Metallocene catalysts and Cp_2MR^+ chemistry: (a) Jordan, R. F. *Adv. Organomet. Chem.* **1991**, *32*, 325. (b) Marks, T. J. *Acc. Chem. Res.* **1992**, *25*, 57. (c) Eisch, J. J.; Piotrowski, A. M.; Brownstein, S. K.; Gabe, E. J.; Lee, F. L. *J. Am. Chem. Soc.* **1985**, *107*, 7219. (d) Hlatky, G. G.; Turner, H. W.; Eckman, R. R. *J. Am. Chem. Soc.* **1989**, *111*, 2728. (e) Jordan, R. F.; Bajgur, C. S.; Willett, R.; Scott, B. *J. Am. Chem. Soc.* **1986**, *109*, 7410. (f) Giannetti, E.; Nicoletti, G. M.; Mazzocchi, R. *J. Polym. Sci., Part A: Polym. Chem. Ed.* **1985**, *23*, 2117. (g) Dyachkovskii, F. S.; Shilova, A. J.; Shilov, A. E. *J. Polym. Sci.* **1967**, *16*, 2333. (h) Thayer, A. M. *Chem. Eng. News* **1995**, *73* (37), 15. (i) Brintzinger, H. H.; Fischer, D.; Mülhaupt, R.; Rieger, B.; Waymouth, R. M. *Angew. Chem., Int. Ed. Engl.* **1995**, *34*, 1143. (j) Sinclair, K. B.; Wilson, R. B. *Chem. Ind.* **1994**, 857. (k) Möhring, P. C.; Coville, N. J. *J. Organomet. Chem.* **1994**, *479*, 1. (l) Horton, A. D. *Trends Polym. Sci.* **1994**, *2*, 158. (m) Bochmann, M. *Nachr. Chem., Tech. Lab.* **1993**, *41*, 1220. (n) Ewen, J. A.; Elder, M. J.; Jones, R. L.; Haspelagh, L.; Atwood, J. L.; Bott, S. G.; Robinson, K. *Makromol. Chem., Macromol. Symp.* **1991**, *48/49*, 253. (o) Bochmann, M. *J. Chem. Soc., Dalton Trans.* **1996**, 255.

$(\text{MeOx})_2\text{Zr}(\text{R})^+$ cations ($\text{R} = \text{CH}_2\text{Ph}$, CH_2CMe_3) adopt distorted square pyramidal structures with a MeOx^- oxygen in the apical position and a *cis*-N arrangement of basal ligands and are inactive for ethylene polymerization. The analogous hafnium $(\text{Ox})_2\text{HfR}_2$ and $(\text{Ox})_2\text{Hf}(\text{R})^+$ compounds exhibit similar behavior.

Here we describe initial studies of related zirconium benzyl complexes of the general type $(\text{pyCR}_2\text{O})_2\text{Zr}(\text{CH}_2\text{Ph})_2$ (Chart 1) and $(\text{pyCR}_2\text{O})_2\text{Zr}(\text{CH}_2\text{Ph})^+$, which incorporate bidentate pyridine–alkoxide ancillary ligands. The objectives of this study were to determine how the increased flexibility of the pyCR_2O^- ligands (versus MeOx^- and MeBr_2Ox^-) influences the structures, dynamics, and olefin reactivity of the resulting metal complexes. Of particular interest is the possibility of tuning reactivity by variation of the substituents on the

Chart 2

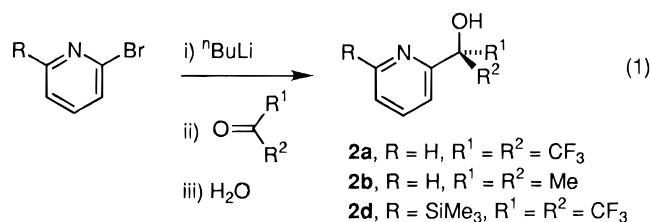


alkoxide carbon and the pyridine ring. Pyridine–alkoxide ligands have been used previously as ancillary ligands in Mo(VI) oxo transfer systems, W(VI) olefin metathesis catalysts, and other complexes.^{3–5}

Results

Ligand Design and Synthesis. The pyCR₂O[–] ligands utilized in this work are listed in Chart 2. Ligands **1a** and **1b** were chosen to probe the influence of ligand electron-donating ability on the chemistry of the target alkyl complexes. The p*K*_a values of the analogous alcohols (CF₃)₂HCOH (9.3) and Me₃COH (20.5) differ by more than 10 units. The chiral ligand **1c** was used to study the stereochemistry and dynamic behavior of metal complexes. Ligand **1d** was designed to suppress electron donation from the pyridine function via front strain (i.e., steric crowding) due to the *ortho*-SiMe₃ substituent.

The reaction of 2-lithiopyridine reagents⁶ with aldehydes or ketones provides general access to pyCR₂O[–] ligands (eq 1).⁷ The reaction of 2-lithiopyridine (from



2-bromopyridine and *n*-BuLi) with hexafluoroacetone or acetone at –78 °C yields pyC(CF₃)₂OLi (**1a**) or pyCMe₂OLi (**1b**), which can be hydrolyzed to alcohols **2a** and **2b**. Deprotonation of **2a** and **2b** (*n*-BuLi) affords **1a** and **1b** as white solids of sufficient purity for use in further reactions. Similarly, the reaction of 2-lithio-6-trimethylsilylpyridine with hexafluoroacetone yields **1d**, which is isolated as a white solid by recrystallization from Et₂O

(3) Schultz, B. E.; Gheller, S. F.; Muetterties, M. C.; Scott, M. J.; Holm, R. H. *J. Am. Chem. Soc.* **1993**, *115*, 2714.

(4) (a) van der Schaaf, P. A.; Abbenhuis, R. A. T. M.; van der Noort, W. P. A.; de Graaf, R.; Grove, D. M.; Smeets, W. J. J.; Spek, A. L.; van Koten, G. *Organometallics* **1994**, *13*, 1433. (b) van der Schaaf, P. A.; Boersma, J.; Smeets, W. J. J.; Spek, A. L.; van Koten, G. *Inorg. Chem.* **1993**, *32*, 5108.

(5) (a) Nietlispach, D.; Veghini, D.; Berke, H. *Helv. Chim. Acta* **1994**, *77*, 2197. (b) van der Schaaf, P. A.; Wissing, E.; Boersma, J.; Smeets, W. J. J.; Spek, A. L.; van Koten, G. *Organometallics* **1993**, *12*, 3624. (c) Van der Zeijden, A. A. H.; Berke, H. *Helv. Chim. Acta* **1992**, *75*, 513. (d) Visalakshi, R.; Jain, V. K.; Kulshreshtha, S. K.; Rao, G. S. *Ind. J. Chem.* **1989**, *28A*, 767. (e) Hiraki, K.; Katayama, R.; Yamaguchi, K.; Honda, S. *Inorg. Chim. Acta* **1982**, *59*, 11. (f) Harrison, P. G.; Phillips, R. C. *J. Organomet. Chem.* **1975**, *99*, 79.

(6) (a) Malmberg, H.; Nilsson, M. *Tetrahedron* **1986**, *42*, 3981. (b) Parham, W. E.; Piccirilli, R. M. *J. Org. Chem.* **1977**, *42*, 257. (c) Gilman, H.; Spatz, S. M. *J. Am. Chem. Soc.* **1940**, *62*, 446.

(7) (a) Taylor, S. L.; Lee, D. Y.; Martin, J. C. *J. Org. Chem.* **1983**, *48*, 4156. (b) Luz, W. D.; Fallab, S.; Erlenmeyer, H. *Helv. Chim. Acta* **1955**, *38*, 1114. (c) Wibaut, J. P.; DeJonge, A. P.; Van der Voort, H. G. P.; Otto, P. Ph. H. L. *Recl. Trav. Chim. Pays-Bas* **1951**, *70*, 1054.

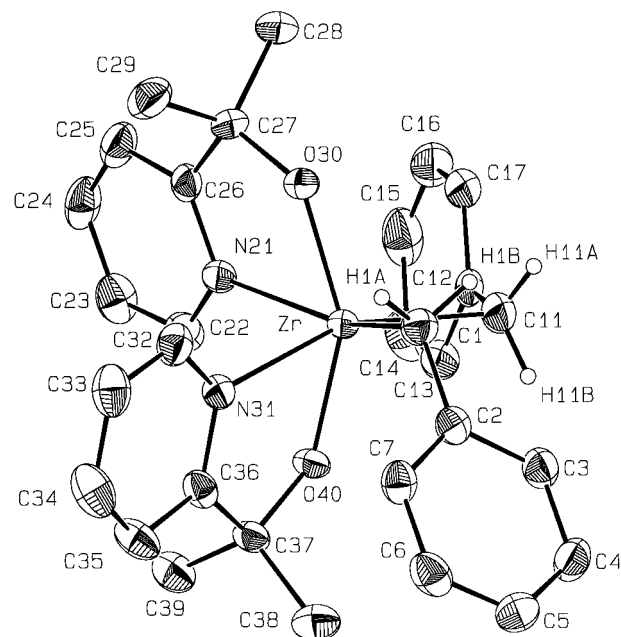
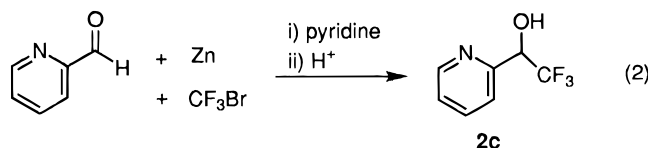


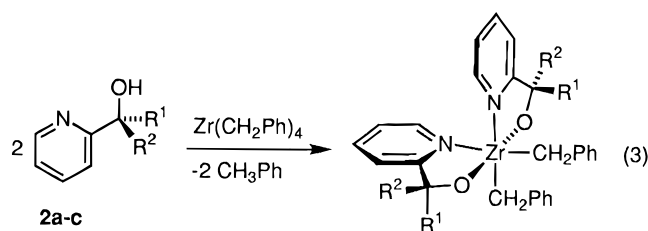
Figure 1. Molecular structure of (pyCMe₂O)₂Zr(CH₂Ph)₂ (**3b**).

and can be hydrolyzed to **2d**. Compound **2c**, pyCH(CF₃)OH, was prepared by Wakselman's method (eq 2).⁸



Synthesis of (pyCR¹R²O)₂Zr(CH₂Ph)₂ Complexes.

The reactions of pyridine alcohols **2a–c** with Zr(CH₂Ph)₄ in toluene or benzene solution result in toluene elimination and yield orange solutions from which (pyCR¹R²O)₂Zr(CH₂Ph)₂ (**3a–c**, eq 3) are isolated in good yield as yellow to orange solids by precipitation with hexane or pentane. The hexafluoro derivative **3a**



3a, R¹ = R² = CF₃

3b, R¹ = R² = Me

3c, R¹, R² = H, CF₃

is highly soluble in aromatic and chlorinated solvents, whereas **3b** and **3c** are less soluble in aromatic solvents.

Solid State Structure of 3b. An X-ray diffraction study was performed on **3b** to determine the metal geometry and the structure of the benzyl groups. Single crystals were obtained from a CH₂Cl₂ solution at –35 °C. An ORTEP view is shown in Figure 1, and crystallographic details and key bond distances and angles are listed in Tables 1–2. Complex **3b** adopts a distorted octahedral structure in which the alkoxide ligands are

(8) Tordeux, M.; Francesc, C.; Wakselman, C. *J. Chem. Soc., Perkin Trans. 1* **1990**, 1951.

Table 1. Summary of Crystallographic Data for (pyCMe₂O)₂Zr(CH₂Ph)₂ (3b)

compound	(pyCMe ₂ O) ₂ Zr(CH ₂ Ph) ₂ (3b)
empirical formula	C ₃₀ H ₃₄ N ₂ O ₂ Zr
fw	545.8
cryst size (mm)	0.44 × 0.47 × 0.49
color/shape	orange/irregular octahedron
space group	<i>P</i> ₂ ₁ / <i>n</i>
<i>a</i> (Å)	10.277(2)
<i>b</i> (Å)	21.958(5)
<i>c</i> (Å)	12.006(3)
β (deg)	93.48(2)
<i>V</i> (Å ³)	2704(2)
<i>Z</i>	4
<i>D</i> _{calc} (g/cm ³)	1.34
temperature (K)	291
diffractometer	Enraf-Nonius CAD-4
diffraction geometry	bisecting
radiation, λ	Mo K α , 0.710 73 Å
monochromator	graphite
2 θ range (deg)	4 < 2 θ < 50
data collected <i>h</i> , <i>k</i> , <i>l</i>	-12 to 3, -1 to 26, -14 to 14
total no. of reflns collected	5754
no. of unique reflns	4606
<i>R</i> _{int}	0.027
obs reflns, criterion	2575 > 3 σ (<i>I</i>)
μ (cm ⁻¹)	4.26
abs corr factors (min/max)	1.000/1.041
abs corr method	ψ scans
structure solution	direct methods ^a
refinement	FMLS on F; non-H, anisotropic; ^b H bonded to sp ³ C, isotropic; H bonded to sp ² C, calculated
<i>R</i>	0.0327 ^c
<i>R</i> _w	0.0433 ^d
max residual density (e/Å ³)	0.35

^a Main, P.; Fiske, S. J.; Hull, S. E.; Lessinger, L.; Germain, G.; DeClercq, J. P.; Woolfson, M. M. *Multan80*; University of York: York U.K., 1980. ^b Data processing and refinement with MolEN. Fair, C. K. *An Interactive System for Crystal Structure Analysis*; Enraf Nonius: Delft, Netherlands, 1990. ^c $R = \sum(|F_o| - |F_c|)/\sum F_o$. ^d $R_w = \{[\sum(F_o - F_c)^2]/[\sum w(F_o)^2]\}^{1/2}$.

trans and the pyridine and benzyl ligands are *cis*. The *cis* L–M–L angles associated with the chelated pyridine–alkoxide ligands are acute (69.2(1)° and 70.1(1)°), while several *cis* angles involving the benzyl ligands are obtuse (N(21)–Zr–C(11), 112.2(1)°; O(30)–Zr–C(11), 104.5(2)°; O(40)–Zr–C(1), 109.6(1)°). These effects can be ascribed to the constraints imposed by the chelation and to benzyl/pyridine–alkoxide steric interactions. The *trans* L–M–L angles range from 149.9(1)° (O(30)–Zr–O(40)) to 156.1(1)° (N(21)–Zr–C(1)).

The Zr–O–C units in **3b** are bent (Zr–O–C angles 132.4(3)°, 130.9(2)°). The Zr–O distances (1.995(3), 2.004(3) Å) are in the range (ca. 1.95–2.08 Å) observed for Cp₂Zr(OR)₂ and Cp₂Zr(OAR)₂ complexes,^{9,10} and are longer than those in highly electron-deficient species such as (triox)₂ZrCl₃Li(OEt)₂,¹¹ *trans*-1,2-(Cl₃(THF)₂-ZrO)₂-cyclohexane,¹² and Zr(O^tBu)₃Si(SiMe₃)₃ (1.86–1.9 Å).¹³ The Zr–O distances in **3b** are slightly shorter than those in (MeOx)₂Zr(CH₂Ph)₂ (2.05 Å). It is reasonable to describe the oxygens in **3b** as sp²-hybridized and to regard the alkoxides as four-electron (σ , π) donors. The five-membered chelate rings are flat to within 0.05

(9) Howard, W. A.; Trnka, T. M.; Parkin, G. *Inorg. Chem.* **1995**, *34*, 5900.

(10) Stephan, D. W. *Organometallics* **1990**, *9*, 2718.

(11) Lubben, T. V.; Wolczanski, P. T.; Van Duyne, G. D. *Organometallics* **1984**, *3*, 977.

(12) Galeffi, B.; Simard, M.; Wuest, J. D. *Inorg. Chem.* **1990**, *29*, 955.

(13) Heyn, R. H.; Tilley, T. D. *Inorg. Chem.* **1989**, *28*, 1768.

Table 2. Selected Bond Distances (Å) and Angles (deg) for (pyCMe₂O)₂Zr(CH₂Ph)₂ (3b)

Zr–O(30)	1.995(3)	O(30)–C(27)	1.410(5)
Zr–O(40)	2.004(3)	O(40)–C(37)	1.410(5)
Zr–N(21)	2.429(3)	C(1)–C(2)	1.483(6)
Zr–N(31)	2.391(3)	C(11)–C(12)	1.461(6)
Zr–C(1)	2.334(4)	C(37)–C(38)	1.525(7)
Zr–C(11)	2.307(5)	C(37)–C(39)	1.528(6)
O(30)–Zr–O(40)	149.9(1)	N(31)–Zr–C(11)	154.6(1)
O(30)–Zr–N(21)	69.2(1)	C(1)–Zr–C(11)	85.2(2)
O(30)–Zr–N(31)	94.6(1)	Zr–O(30)–C(27)	132.4(3)
O(30)–Zr–C(1)	91.2(1)	Zr–O(40)–C(37)	130.9(2)
O(30)–Zr–C(11)	104.5(2)	Zr–N(21)–C(22)	127.1(3)
O(40)–Zr–N(21)	84.7(1)	Zr–N(21)–C(26)	114.8(3)
O(40)–Zr–N(31)	70.1(1)	C(22)–N(21)–C(26)	118.0(4)
O(40)–Zr–C(1)	109.6(1)	Zr–N(31)–C(32)	125.9(3)
O(40)–Zr–C(11)	98.9(1)	Zr–N(31)–C(36)	114.5(3)
N(21)–Zr–N(31)	90.1(1)	C(32)–N(31)–C(36)	119.3(4)
N(21)–Zr–C(1)	156.1(1)	Zr–C(1)–C(2)	116.6(3)
N(21)–Zr–C(11)	112.2(1)	Zr–C(11)–C(12)	96.1(3)
N(31)–Zr–C(1)	77.6(1)		

Å and appear not to be significantly strained.¹⁴ The Zr–N(21)–C(26) angle (114.8(3)°) is 12° smaller than the Zr–N(21)–C(2) angle (127.1(3)°); i.e., the Zr center is displaced ca. 6° toward O(30) from the orientation which would maximize the N–Zr donor interaction. A similar effect is observed in the other chelate ring. The Zr–N distances (2.429(3), 2.391(3) Å) are at the long end of the range observed for Zr(IV) complexes of simple and chelated pyridine ligands (2.3–2.4 Å),¹⁵ which may reflect the constraints of the chelation and the *trans* influence of the benzyl groups.

The C(1)–C(7) benzyl ligand of **3b** has a normal structure (Zr–C(1)–C(2) angle 116.6(3)°), while the C(11)–C(17) benzyl ligand exhibits a small Zr–C(11)–C(12) angle (96.1(3)°) and a nonbonded Zr–C_{ipso} distance of 2.86 Å. These features imply the presence of a weak Zr···Ph interaction (i.e., (η^2 -benzyl)), as commonly observed for electron deficient metal benzyl complexes.^{16,17} The C(11)–C(17) benzyl is structurally similar to the distorted benzyl in Zr(CH₂Ph)₄(dmpe) (Zr–C–C, 94.2(4)°; Zr–C_{ipso} 2.788(8) Å),^{16e} but it is much less distorted than

(14) In systems of this type, chelate ring strain is expected to be relieved by adjustment of the Zr–O–C angle. The potential surface for Zr–O–C bending is probably quite flat.

(15) (a) Howard, W. A.; Parkin, G. *J. Am. Chem. Soc.* **1994**, *116*, 606. (b) Moore, E. J.; Straus, D. A.; Armantrout, J.; Santarsiero, B. D.; Grubbs, R. H.; Bercaw, J. E. *J. Am. Chem. Soc.* **1983**, *105*, 2068. (c) Arnold, J.; Woo, H.-G.; Tilley, T. D. *Organometallics* **1988**, *7*, 2045. (d) Jordan, R. F.; Taylor, D. F.; Baenziger, N. C. *Organometallics* **1990**, *9*, 1546.

(16) (a) Davies, G. R.; Jarvis, J. A. J.; Kilbourn, B. T.; Pioli, A. J. P. *J. Chem. Soc., Chem. Commun.* **1971**, 677. (b) Davies, G. R.; Jarvis, J. A. J.; Kilbourn, B. T. *J. Chem. Soc., Chem. Commun.* **1971**, 1511. (c) Bassi, I. W.; Allegra, G.; Scordamaglia, R.; Chiccola, G. *J. Am. Chem. Soc.* **1971**, *93*, 3787. (d) Mintz, E. A.; Moloy, K. G.; Marks, T. J.; Day, V. W. *J. Am. Chem. Soc.* **1981**, *104*, 4692. (e) Girolami, G. S.; Wilkinson, G.; Thornton-Pett, M.; Hursthouse, M. B. *J. Chem. Soc., Dalton Trans.* **1984**, 2789. (f) Edwards, P. G.; Andersen, R. A.; Zalkin, A. *Organometallics* **1984**, *3*, 293. (g) Latesky, S. L.; McMullen, A. K.; Nicolai, G. P.; Rothwell, I. P.; Huffman, J. C. *Organometallics* **1985**, *4*, 902. (h) Jordan, R. F.; LaPointe, R. E.; Bajgur, C. S.; Echols, S. F.; Willet, R. *J. Am. Chem. Soc.* **1987**, *109*, 4111. (i) Scholz, J.; Schlegel, M.; Thiele, K. H. *Chem. Ber.* **1987**, *120*, 1369. (j) Jordan, R. F.; LaPointe, R. E.; Baenziger, N.; Hinch, G. D. *Organometallics* **1990**, *9*, 1539. (k) Alelyunas, Y. W.; Jordan, R. F.; Echols, S. F.; Borkowsky, S. L.; Bradley, P. K. *Organometallics* **1991**, *10*, 1406. (l) Dryden, N. H.; Legzdins, P.; Trotter, J.; Yee, V. C. *Organometallics* **1991**, *10*, 2857. (m) Hughes, A. K.; Meetsma, A.; Teuben, J. H. *Organometallics* **1993**, *12*, 1936. (n) Pellecchia, C.; Immirzi, A.; Pappalardo, D.; Peluso, A. *Organometallics* **1994**, *13*, 3773.

(17) It is also possible that π – π stacking interactions between the C(12)–C(17) phenyl ring and the C–C pyridine contribute to the small Zr–C(11)–C(12) angle. There are several short inter-ring distances (Å): C(13)–C(22), 3.55; C(14)–C(22), 3.52; C(17)–C(22), 3.95; C(17)–C(23), 3.95.

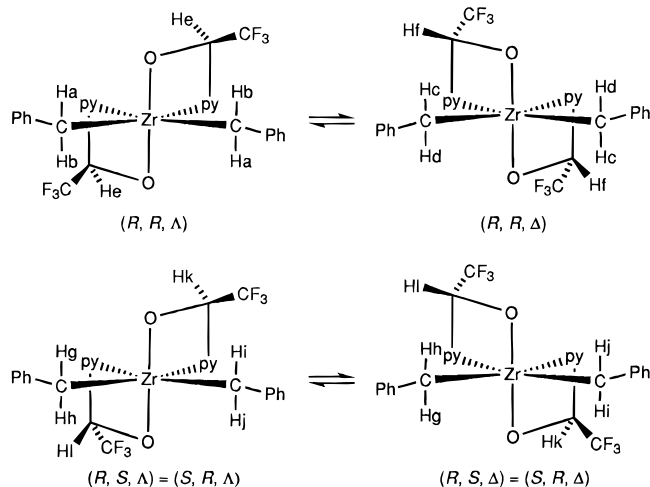


Figure 2. Schematic structures, stereochemical descriptors, and interconversion of the stereoisomers of $\{\text{pyCH}(\text{CF}_3)\text{O}\}_2\text{Zr}(\text{CH}_2\text{Ph})_2$ (**3c**).

those in cationic complexes such as $\text{Cp}_2\text{Zr}(\text{CH}_2\text{Ph})(\text{CH}_3\text{CN})^+$ ($\text{Zr}-\text{C}-\text{C}$, 84.9(4)°; $\text{Zr}-\text{C}_{\text{ipso}}$, 2.648(6) Å) or $(\text{C}_5\text{Me}_5)\text{Zr}(\text{CH}_2\text{Ph})_2^+$ (η^7 -benzyl, $\text{Zr}-\text{C}-\text{C}$, 62.1(2)°; $\text{Zr}-\text{C}_{\text{ipso}}$ 2.349(3) Å).¹⁶ⁿ There are no close $\text{Zr}-\text{H}_\alpha$ contacts ($\text{Zr}-\text{H}_\alpha > 2.67$ Å).

Overall, **3b** is best described as a 16-electron species (counting the alkoxides as 4-electron donors), which may be stabilized to some extent by the weak $\text{Zr}\cdots\text{Ph}$ interaction. The structure of **3b** is very similar to that of $(\text{MeOx})_2\text{Zr}(\text{CH}_2\text{Ph})_2$, which was described in the previous paper in this series.¹

Solution Structure and Dynamics of 3c. (i) Isomer Possibilities. To elucidate the solution structures and dynamic properties of **3a–c**, we first investigated the variable-temperature NMR spectra of **3c**. Neglecting for the moment the possibility of η^2 -benzyl interactions, three diastereomers and with the same metal geometry as that in the solid state structure of **3b** are possible for **3c**, as illustrated in Figure 2; these isomers may be denoted by the descriptors (R, R, Λ) , (R, R, Δ) , and $(R, S, \Lambda) = (S, R, \Lambda)$, where the first two entries specify the configurations of the “top” and “bottom” alkoxide carbons and the third specifies that of the metal.

The C_2 symmetric (R, R, Λ) and (R, R, Δ) diastereomers differ in the orientation of the CF_3 groups; in the former both point toward the benzyl ligands, while in the latter both point away from these groups.¹⁸ The metal configurations of these isomers also differ. For each of these isomers, two doublets for the ZrCH_2 hydrogens (H_a and H_b ; H_c and H_d) and a quartet for the CHCF_3 hydrogens (H_e ; H_f , J_{CF}) are expected in the ^1H NMR spectrum.

The (R, S, Λ) and (S, R, Λ) isomers are related by a 180° rotation about the axis which bisects the $\text{C}-\text{Zr}-\text{C}$ angle and are thus identical, as indicated in Figure 2. The enantiomers, (S, R, Δ) and (R, S, Δ) , are related in the same way. The ^1H NMR spectrum of the (R, S, Λ) diastereomer should contain four doublets for the ZrCH_2 hydrogens (H_g , H_h , H_i , H_j) and two quartets for the CHCF_3 hydrogens (H_k , H_l).

Inversion of the metal configuration would result in interconversion of the (R, R, Λ) and (R, R, Δ) diaster-

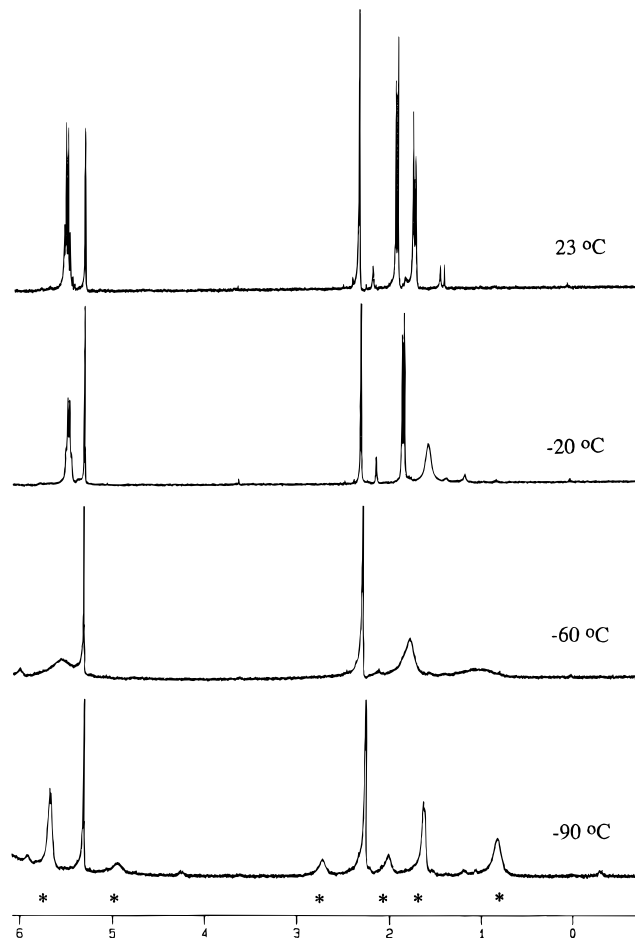


Figure 3. Variable-temperature ^1H NMR spectra of a sample of $\{\text{pyCH}(\text{CF}_3)\text{O}\}_2\text{Zr}(\text{CH}_2\text{Ph})_2$ (**3c**) enriched in the (R, R, Λ) and (R, R, Δ) isomers. The resonances for these species are labeled by asterisks and are noted in the text. The remaining resonances are due to CH_2Cl_2 (δ 5.32), toluene (δ 2.30), and the (R, S, Λ) isomer of **3c**.

eomers and racemization of the (R, S, Λ) isomer. However, interconversion of the (R, R, Λ) and (R, R, Δ) isomers with the (R, S, Λ) isomer requires intermolecular exchange of pyridine–alkoxide ligands, due to the different alkoxide carbon configurations.

(ii) (R, R, Λ) and (R, R, Δ) Diastereomers. The sample of **3c** isolated from eq 3 consists of a mixture of the (R, R, Λ) and (R, R, Δ) diastereomers (93% total, NMR) and a small amount of the (R, S, Λ) isomer (7%). Variable-temperature ^1H NMR spectra of this sample (CD_2Cl_2) are shown in Figure 3. The ^1H NMR spectrum of the (R, R, Λ) and (R, R, Δ) isomers at -90 °C contains four broad resonances (δ 2.73, 2.01, 1.65, 0.83) for the ZrCH_2 hydrogens (H_a , H_b , H_c , H_d in Figure 2) and two broad resonances (δ 5.68, 4.95) for the CHCF_3 hydrogens (H_e , H_f). The ratio of the two isomers is 3/1 at -90 °C based on integration of the ZrCH_2 resonances. These observations are consistent with the structures in Figure 2; while the isomers cannot be assigned, it is expected that the (R, R, Λ) isomer would be disfavored by CF_3 /benzyl steric interactions. The broadness of these resonances may be due to the incomplete freezing out of the exchange process shown in Figure 2 or more likely to rapid exchange of η^2 - and η^1 -benzyl groups. At -60 °C, the ZrCH_2 resonances collapse to two broad signals (δ 1.79, 1.08) and the CHCF_3 resonances coalesce into a broad signal (δ 5.56). At 23 °C, two sharp

(18) The enantiomer configurations are (S, S, Δ) , (S, S, Λ) .

doublets (δ 1.94, 1.75; $J = 8.6$ Hz) are observed for the ZrCH_2 hydrogens and a sharp quartet (δ 5.52, $J_{\text{CF}} = 7.4$ Hz) is observed for the CHCF_3 hydrogens. These observations are consistent with rapid (NMR time scale) inversion of configuration at Zr above -60 °C (i.e., rapid interconversion of the (*R, R, \Lambda*) and (*R, R, \Delta*) isomers), which exchanges Ha with Hc, Hb with Hd, and He with Hf, as shown in Figure 2.¹⁹ The barrier estimated for this exchange process from the coalescence of the CHCF_3 signals is ΔG^\ddagger (major to minor) = 10.1(3) kcal/mol.²⁰

The presence of one weakly distorted and one normal benzyl ligand in the solid state structure of **3b** suggests that distorted benzyl ligands are possible in **3c** as well. Distorted $\text{M}-\text{CH}_2\text{Ph}$ groups can be detected by ^1H and ^{13}C NMR spectroscopy; in particular, the reduction of the $\text{M}-\text{C}-\text{C}$ angle and concomitant increase in $\text{H}-\text{C}-\text{H}$ angle which result from $\text{M}\cdots\text{Ph}$ interactions are manifested by reduced J_{HH} values ($< \text{ca. } 10$ Hz) and large J_{CH} values ($> \text{ca. } 125$ Hz).¹⁶ The J_{HH} and J_{CH} values of **3c** are 8.6 and 130 Hz, respectively. These values, which are averages for the four unique benzyl groups in the two isomers, indicate that the benzyl groups are distorted to some degree in solution. Given the structure of **3b**, it is likely that the (*R, R, \Lambda*) and (*R, R, \Delta*) isomers of **3c** each contain one distorted and one normal benzyl group which undergo rapid exchange.

(iii) (*R, S, \Lambda*) Isomer. When the solution of **3c** described above, which was enriched in the (*R, R, \Lambda*) and (*R, R, \Delta*) isomers, was allowed to stand at 23 °C for 9 h, the (*R, S, \Lambda*) = (*R, S, \Delta*) diastereomer grew in at the expense of the (*R, R, \Lambda*) and (*R, R, \Delta*) isomers. The final isomer ratio $\{(\text{R, R, } \Lambda) + (\text{R, R, } \Delta)\}/(\text{R, S, } \Lambda)$ was 46/54. As noted above, this isomer exchange requires intermolecular exchange of the pyridine-alkoxide ligands. The ^1H NMR spectra of this mixture (Figure 4) contain resonances for the (*R, R, \Lambda*) and (*R, R, \Delta*) isomers (for which the intensity ratio and temperature dependence are identical to those observed for the sample enriched in those isomers) and resonances for the (*R, S, \Lambda*) isomer, which will be described here.²¹ At -90 °C, the spectrum of the (*R, S, \Lambda*) isomer contains four doublets (δ 2.23, 2.02, $J_{\text{HH}} = 6.8$ Hz; 1.20, -0.30 , $J_{\text{HH}} = 8.3$ Hz) for the ZrCH_2 hydrogens (Hg, Hh, Hi, Hj) and two quartets (δ 5.92, 4.23) for the CHCF_3 hydrogens (Hk, Hl), as expected from Figure 2. At -60 °C, the two low-field ZrCH_2 resonances coalesce to a broad signal (δ 2.13). As the temperature is raised, the two high-field ZrCH_2 resonances shift downfield, coalesce to a broad signal at δ 1.03 at -40 °C, and sharpen to a sharp singlet at δ 1.46 at 20 °C. The CHCF_3 resonances coalesce to a sharp quartet (δ 5.49) as the temperature is raised; however, this change is partially masked by the temperature-dependent CHCF_3 resonances of the (*R, R, \Lambda/\Delta*) isomers. These results are consistent with rapid (NMR time scale) racemization of

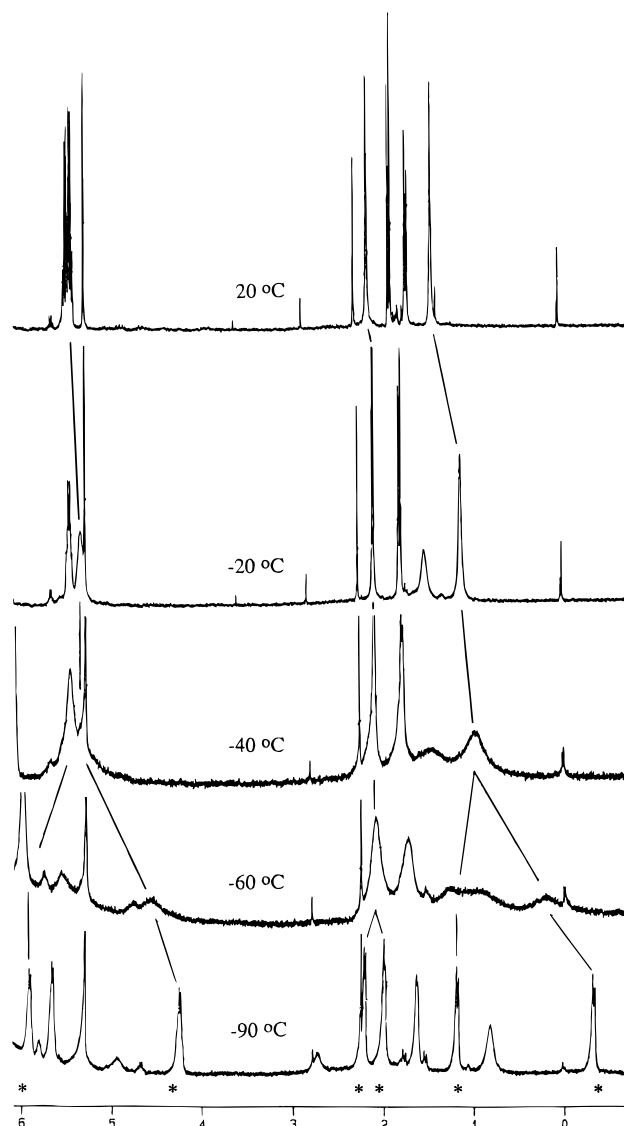


Figure 4. Variable-temperature ^1H NMR spectra of a sample of **3c** enriched in the (*R, S, \Lambda*) isomer. The resonances for this species are labeled by asterisks, and the temperature dependence of these resonances is indicated by the vertical lines. The remaining resonances are due to the (*R, R, \Lambda*) and (*R, R, \Delta*) isomers of **3c**, CH_2Cl_2 , toluene, and minor impurities.

the (*R, S, \Lambda*) isomer, which results in exchange of Hg and Hh, exchange of Hi and Hj, and exchange of Hk and Hl (Figure 2). A barrier ΔG^\ddagger (racemization) = 10.1(2) kcal/mol is estimated from the coalescence of the low-field ZrCH_2 doublets.

The ZrCH_2 J_{HH} (6.8, 8.3 Hz; -90 °C) and J_{CH} (132, 127 Hz; 23 °C) values indicate that the two unique benzyl ligands of the (*R, S, \Lambda*)/(*R, S, \Delta*) isomer are both distorted to some degree. These data can be accommodated by a structure which contains one normal and one distorted benzyl (as observed for **3b** in the solid state) which undergo rapid exchange. The spread in the J_{HH} and J_{CH} values indicates that the η^2 -interaction is more favored for one benzyl than the other. Steric crowding due to the proximal CF_3 group may disfavor a $\text{Zr}\cdots\text{Ph}$ interaction involving the $-\text{CH}_2\text{H}_2\text{Ph}$ benzyl (Figure 2). The origin of the large temperature dependence of the chemical shifts of the high-field ZrCH_2 resonances is unknown.²²

(19) The downfield shift of the ZrCH_2 resonances with increasing temperature may be related to changes in the ZrCH_2Ph conformation.

(20) (a) This barrier was estimated using the graphical method described in Shanan-Atidi, H.; Bar-Eli, K. H. *J. Phys. Chem.* **1970**, *74*, 961. (b) ΔG^\ddagger (minor to major) = 9.6(3) kcal/mol.

(21) The ^{13}C NMR spectrum of the (*R, R, \Lambda*), (*R, R, \Delta*), (*R, S, \Lambda*) mixture at 23 °C contains one set of pyridine and benzyl resonances for the rapidly exchanging (*R, R, \Lambda*) and (*R, R, \Delta*) isomers and one set of pyridine resonances and two sets of benzyl resonances for the rapidly racemizing (*R, S, \Lambda*) isomer.

(iv) Summary. On the basis of these NMR results, it is concluded that (i) the static structures for the three isomers of **3c** are similar to the solid state structure of **3b**, i.e., the alkoxide groups are *trans*, the pyridine ligands are *cis*, and the benzyl ligands are *cis*; (ii) inversion of configuration at Zr occurs rapidly on the NMR time scale at 23 °C, probably via a five-coordinate intermediate formed by reversible pyridine dissociation;¹ and (iii) intermolecular ligand exchange occurs slowly (hours) on the lab time scale. Additionally, (iv) in the static structure of **3c**, one benzyl group is probably distorted (η^2); however, exchange of the distorted and normal benzyl groups is rapid on the NMR time scale even at -90 °C.

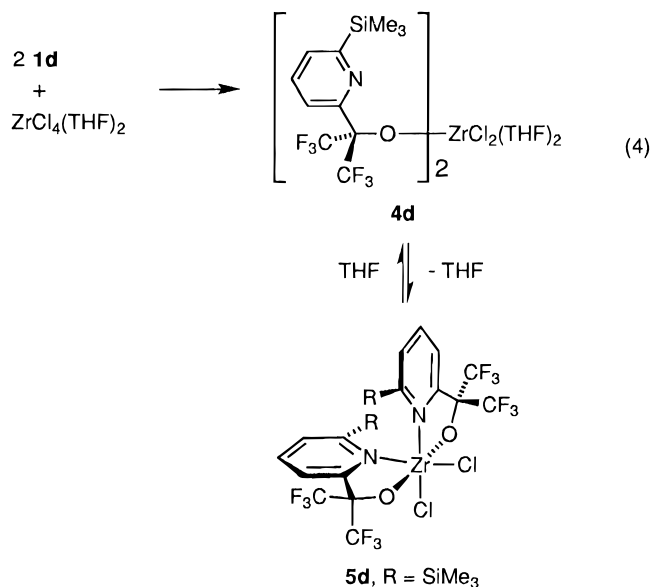
Solution Structure and Dynamics of 3b. The ¹H NMR spectrum of **3b** at -100 °C contains a single set of pyridine and benzyl aryl resonances (several of which are broad), two broad singlets for the alkoxide methyl groups, and two broad singlets for the benzyl methylene hydrogens. This pattern is consistent with the metal geometry observed for **3b** in the solid state, in which the Me groups are inequivalent and the ZrCH₂ hydrogens are diastereotopic.²³ At -90 °C, the Me resonances and the ZrCH₂ resonances collapse to singlets, and above -20 °C, all of the resonances are sharp. These observations establish that **3b** undergoes rapid inversion of the configuration at Zr. The barrier to this process determined from the coalescence of the Me signals is $\Delta G^\ddagger = 8.6(2)$ kcal/mol. The bonding mode(s) of the benzyl ligands for **3b** in solution cannot be unambiguously determined from the NMR data. However, in view of the solid state structure, the broadening of the pyridine and benzyl aryl resonances at low temperature may be ascribed to rapid exchange of one normal and one weakly distorted benzyl ligand. The ZrCH₂ J_{CH} value observed in the ambient-temperature ¹³C spectrum of **3b** is normal (121 Hz). This value is the average for the two benzyl groups, and little deviation from the normal range is expected for a case where one benzyl ligand is normal and one is only slightly distorted.

Solution Structure and Dynamics of 3a. The variable-temperature NMR properties of **3a** are similar to those of **3b** and **3c**. The ambient-temperature ¹H NMR spectrum contains a single set of pyridine and benzyl aryl resonances and a sharp singlet for the ZrCH₂ hydrogens. As the temperature is lowered to -100 °C, the benzyl aryl resonances broaden and the ZrCH₂ resonance splits to two singlets. These observations are consistent with a static structure analogous to the solid state structure of **3b** and rapid inversion of configuration at Zr. The inversion barrier calculated from the coalescence of the ZrCH₂ signals ($\Delta G^\ddagger = 8.8(2)$ kcal/mol) is very similar to that for **3b**.²⁴ The ZrCH₂ J_{CH} value determined at 23 °C (125 Hz), which is the average

value for the two benzyl groups, is slightly higher than that observed for **3b**, which suggests that the degree of benzyl group distortion may be higher.

Attempted Syntheses of {pyC(CF₃)₂O}₂ZrCl₂. The dichloride complex {pyC(CF₃)₂O}₂ZrCl₂ is a potential general precursor to {pyC(CF₃)₂O}₂ZrR₂ complexes. However, to date it has not been possible to synthesize this species. The reaction of ZrCl₄ or ZrCl₄(THF)₂ and 2 equiv of LiOC(CF₃)₂py (**1a**) in toluene, hexane, or Et₂O under a variety of conditions yields mixtures in which the tris(ligand) complex {pyC(CF₃)₂O}₃ZrCl is a major component. The reaction of ZrCl₄ and 3 equiv of **1a** in Et₂O yields {pyC(CF₃)₂O}₃ZrCl cleanly. This species was not studied further.

Synthesis of {6-SiMe₃-pyC(CF₃)₂O}₂ZrCl₂ (5d**).** The reaction of ZrCl₄(THF)₂ and 2 equiv of **1d** in hexane yields {6-SiMe₃-pyC(CF₃)₂O}₂ZrCl₂(THF)₂ (**4d**), which is isolated as a white solid (eq 4). The ¹H NMR



spectrum of **4d** contains resonances for coordinated THF. The THF is removed from **4d** at 95 °C (N₂ flow, toluene) to afford base-free {6-SiMe₃-pyC(CF₃)₂O}₂ZrCl₂ (**5d**), which is reconverted to **4d** upon contact with THF. The SiMe₃ ¹H NMR resonance of THF adduct **4d** (0.27, C₆D₆) is not significantly shifted from those of **1d** (δ 0.30, C₆D₆) or the parent alcohol **2d** (δ 0.33, CDCl₃) while that of **5d** is shifted ca. 0.3 ppm downfield (δ 0.64, CD₂Cl₂). This suggests that the pyridine in **4d** is not coordinated. Due to the apparent lability of the bulky *ortho*-disubstituted pyridine, this system was not studied further.

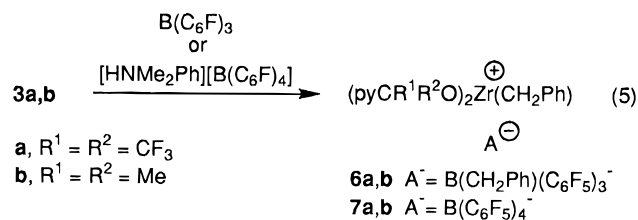
Generation of (pyCR₂O)₂Zr(CH₂Ph)⁺ Species. The reaction of **3a** with B(C₆F₅)₃ in benzene yields [(pyC(CF₃)₂O)₂Zr(CH₂Ph)][(PhCH₂)B(C₆F₅)₃] (**6a**), which separates from the reaction solution as a yellow oil and can be isolated as a yellow solid by washing and vacuum drying (eq 5).²⁵ Similarly, the reaction of **3a** with

(22) The high-field ZrCH₂ shifts may reflect α -agostic interactions. For examples of early metal benzyl complexes with α -agostic interactions, see: (a) Mena, M.; Pellinghelli, M. A.; Royo, P.; Serrano, R.; Tiripicchio, A. *J. Chem. Soc., Chem. Commun.* **1986**, 1118. (b) Booi, M.; Meetsma, A.; Teuben, J. H. *Organometallics* **1991**, *10*, 3246.

(23) A minor isomer of **3b** (15%) is observed at -60 °C and below; NMR data for this species are consistent with a *cis*-O, *cis*-N, *trans*-benzyl structure. ¹H NMR (-90 °C, CD₂Cl₂): δ 8.66 (br d, 2H, 6-py), 7.91 (t, $J = 7.4$ Hz, 2H, 4-py), 7.60 (br t, 2H, 5-py), 7.29 (d, $J = 8$ Hz, 2H, 3-py), 6.62 (t, $J = 7.4$ Hz, 4H, *m*-Ph), 5.92 (d, $J = 7.4$ Hz, *o*-Ph), 1.73 (s, 4H, CH₂), 0.97 (s, 6H, Me), *p*-Ph signal obscured.

(24) The two CF₃ groups on a given pyC(CF₃)₂O- ligand of **3a** are inequivalent in the static structure. The ambient-temperature ¹³C and ¹⁹F NMR spectra contain single resonances for the CF₃ groups. The ¹³C NMR CF₃ resonance does not split as expected down to -80 °C. Presumably, the ¹⁹F and ¹³C chemical shift differences for the inequivalent CF₃ groups are small.

(25) For use of B(C₆F₅)₃ in the generation of Cp₂Zr(R)⁺ species, see ref 2 and Yang, X.; Stern, C. L.; Marks, T. J. *J. Am. Chem. Soc.* **1994**, *116*, 10015 and references therein.



[HNMe₂Ph][B(C₆F₅)₄] in benzene yields the analogous B(C₆F₅)₄⁻ salt [{pyC(CF₃)₂O}₂Zr(CH₂Ph)][B(C₆F₅)₄] (**7a**) in base-free form.²⁶ These cationic species are soluble in CD₂Cl₂ but decompose in several hours at ambient temperature in this solvent.²⁷ Similarly, the reaction of **3b** with B(C₆F₅)₃ or [HNMe₂Ph][B(C₆F₅)₄] yields the analogous salts [(pyCMe₂O)₂Zr(CH₂Ph)][(PhCH₂)B(C₆F₅)₃] (**6b**) and [(pyCMe₂O)₂Zr(CH₂Ph)][B(C₆F₅)₄] (**7b**). Compound **6b** is much more stable in CD₂Cl₂ than the fluorinated analogue **6a**, decomposing only slightly after 48 h at ambient temperature. Attempts to purify and obtain crystalline samples of **6a,b** and **7a,b** were unsuccessful due to poor solubility and thermal stability properties, and therefore, these compounds were characterized by NMR spectroscopy.

Structures of (pyCR₂O)₂Zr(CH₂Ph)⁺ Species. The NMR spectra of **6a** and **7a** in CD₂Cl₂ are identical except for the anion resonances, which indicates that cation–anion interactions are absent or weak in this solvent. The ambient-temperature ¹H NMR spectrum of the {pyC(CF₃)₂O}₂Zr(CH₂Ph)⁺ cation contains a single set of pyridine resonances and a broad singlet for the ZrCH₂ unit. However, the –80 °C spectrum contains two sets of pyridine resonances and an AB pattern for the ZrCH₂ unit and indicates that the sides of the benzyl Ph group are inequivalent. These observations establish that the static structure of {pyC(CF₃)₂O}₂Zr(CH₂Ph)⁺ is unsymmetrical but that this species is fluxional. The ZrCH₂ J_{HH} value (8.2 Hz) and J_{CH} value (142 Hz) indicate that the benzyl ligand is distorted. X-ray crystallographic studies establish that (MeBr₂Ox)₂Zr(η²-CH₂Ph)⁺ (Chart 1)¹ and {pyC(3,5-(CF₃)₂-C₆H₃)₂O}₂Ti(η²-CH₂Ph)⁺,²⁸ which are both closely related to {pyC(CF₃)₂O}₂Zr(η²-CH₂Ph)⁺, adopt distorted square pyramidal structures with an η²-benzyl group in the apical position, the benzyl Ph group aligned over a M–N bond, and a *trans*-O, *trans*-N arrangement of basal ligands. The NMR data for the {pyC(CF₃)₂O}₂Zr(CH₂Ph)⁺ cation are consistent with a static structure of this type (Chart 3).

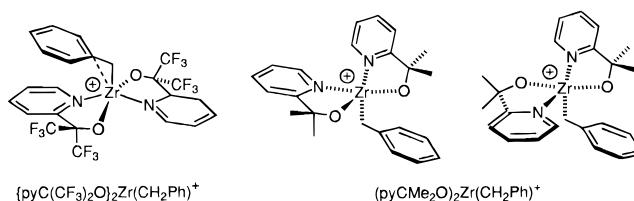
The NMR spectra of **6b** and **7b** in CD₂Cl₂ are identical except for the anion resonances, again indicating that

(26) For use of HNR₃⁺ reagents in the generation of Cp₂Zr(R)⁺ species, see ref 2 and (a) Bochmann, M.; Wilson, L. M. *J. Chem. Soc., Chem. Commun.* **1986**, 1610. (b) Lin, Z.; Le Marechal, J.; Sabat, M.; Marks, T. J. *J. Am. Chem. Soc.* **1987**, *109*, 4127. (c) Turner, H. W.; Hlatky, G. G. Eur. Pat. Appl. 0 277 003, 1988. (d) Turner, H. W. Eur. Pat. Appl. 0 277 004, 1988. (e) Hlatky, G. G.; Eckman, R. R.; Turner, H. W. *Organometallics* **1992**, *11*, 1413. (f) Eshuis, J. J. W.; Tan, Y. Y.; Meetsma, A.; Teuben, J. H.; Renkema, J.; Evens, G. G. *Organometallics* **1992**, *11*, 362. (g) Amorose, D. M.; Lee, R. P.; Petersen, J. L. *Organometallics* **1991**, *10*, 2191. (h) Horton, A. D.; Orpen, A. G. *Organometallics* **1991**, *10*, 3910. (i) Bochmann, M.; Jagger, A. J.; Nicholls, J. C. *Angew. Chem., Int. Ed. Engl.* **1990**, *29*, 780. (j) Horton, A. G.; Frijins, J. H. G. *Angew. Chem., Int. Ed. Engl.* **1991**, *30*, 1152. (k) Grossman, R. B.; Doyle, R. A.; Buchwald, S. L. *Organometallics* **1991**, *10*, 1501. (l) Bochmann, M.; Lancaster, S. J. *J. Organomet. Chem.* **1992**, *434*, C1. (m) Guo, Z.; Swenson, D. C.; Jordan, R. F. *Organometallics* **1994**, *13*, 1424.

(27) ¹H NMR spectra of {pyC(CF₃)₂O}₂ZrCH₂Ph⁺ in CD₂Cl₂ following decomposition are complicated, and the product(s) have not been identified.

(28) (a) Lubben, T.; Nishihara, Y.; Young, V. G., Jr.; Jordan, R. F. Manuscript in preparation.

Chart 3



cation–anion interactions are not significant. The (pyCMe₂O)₂Zr(CH₂Ph)⁺ cation exists as a 3/2 mixture of two isomers which are not fluxional on NMR time scale at ambient temperature. For each isomer, the ¹H NMR spectrum contains four pyCMe₂O resonances and an AB pattern for the ZrCH₂ unit, and the ¹³C NMR spectrum contains four Me signals and two sets of pyCMe₂O signals. Thus, for each isomer, the two pyCMe₂O⁻ ligands are inequivalent, the Me groups on each are inequivalent, and the ZrCH₂ hydrogens are diastereotopic. The Zr–benzyl groups of the two isomers are not significantly distorted by Zr⋯Ph interactions (major isomer J_{HH} = 10.7 Hz, J_{CH} = 126 Hz; minor isomer J_{HH} = 11.2 Hz, J_{CH} = 119 Hz). We showed previously by detailed 1- and 2-D NMR studies that (MeOx)₂Zr(R)⁺ cations (R = CH₂Ph, CH₂CMe₃) adopt distorted square pyramidal structures with a MeOx⁻ oxygen in the apical position, the R group in a basal position, and a *cis*-N arrangement of basal ligands (Chart 1).¹ The NMR data for the two isomers of (pyCMe₂O)₂Zr(CH₂Ph)⁺ are consistent with similar distorted square pyramidal structures, with the benzyl group in a basal position and either an alkoxide or a pyridine ligand in the apical position (Chart 3).

The structural differences between the {pyC(CF₃)₂O}₂Zr(η²-CH₂Ph)⁺ and (pyCMe₂O)₂Zr(CH₂Ph)⁺ cations may be rationalized in terms of electronic effects similar to those invoked in our earlier analysis of the (Ox)₂M(R)⁺ system.¹ Two key features of the proposed structure of {pyC(CF₃)₂O}₂Zr(η²-CH₂Ph)⁺ are (i) the two alkoxide ligands must share a single metal d orbital for p–d π-bonding and (ii) the vacant coordination site is *trans* to the benzyl ligand, which is the strongest *trans*-influence ligand present. As O–Zr π-donation is extremely weak at best for the fluorinated alkoxide, the latter feature controls the structure. In contrast, O–Zr π-donation is more important for (pyCMe₂O)₂Zr(CH₂Ph)⁺, and this species adopts structures in which the alkoxides do not compete for the same d orbital.

Olefin Polymerization Studies. (i) Ethylene Polymerization with Discrete Cationic Complexes.

The ethylene polymerization activities of (pyCR₂O)₂Zr(CH₂Ph)⁺ cations **6a,b** and {pyCH(CF₃)O}₂Zr(CH₂Ph)⁺ (**6c**)²⁹ have been investigated. In an initial series of experiments, **6a–c** were generated *in situ* in benzene via reaction of **3a–c** with B(C₆F₅)₃ and their activities compared under standard conditions (benzene, 40 °C, 3 atm, 30 min polymerization time). The activity varies in the order **6a** (32 (kg of PE)(mol of cat)⁻¹ atm⁻¹ h⁻¹) > **6c** (2.6) > **6b** (no polymer). Thus, for this system, the electron-withdrawing CF₃ groups have a beneficial effect on activity. The polymer produced by **6a** under these conditions is a low molecular weight (M_n = 6,200), linear polyethylene with one vinyl end group per chain; i.e., a C₄₀₀ α-olefin. The molecular weight distribution

(29) Cation **6c** was generated *in situ* only.

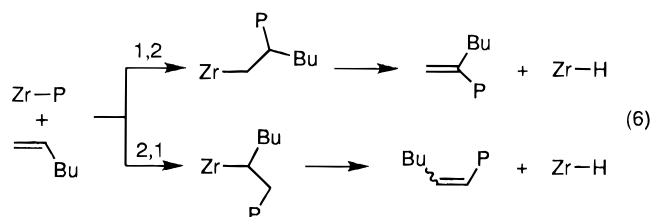
($M_w/M_n = 2.6$) is somewhat broader than that expected for a single site catalyst ($M_w/M_n = 2.0$). Benzyl end groups were also detected by ^1H NMR, suggesting that polymerization is initiated via insertion into the Zr–CH₂Ph bond of **6a** or a Zr benzyl species derived therefrom. These results are in accord with a normal insertion mechanism and efficient chain transfer via β -H elimination.

Activation of **3a** by [HNMe₂Ph][B(C₆F₅)₄] (to generate **7a** and NMe₂Ph) resulted in decreased activity (13 (kg of PE)(mol of cat)⁻¹ atm⁻¹ h⁻¹) under the standard conditions noted above. While NMe₂Ph does not coordinate to **7a** in CH₂Cl₂, it is possible that this Lewis base may compete with ethylene for binding to {pyC(CF₃)₂O}₂Zr(R)⁺ species in benzene. Complex **3a** is also activated efficiently by [Ph₃C][B(C₆F₅)₄] (to generate **7a**); in this case, the activity and polymer properties are similar to those for the **3a**/B(C₅F₅)₃ catalyst (56 (kg of PE)(mol of cat)⁻¹ atm⁻¹ h⁻¹; toluene, 45 °C, 8 atm, 60 min).³⁰ The use of Al(ⁱBu)₃ as a scavenger in conjunction with the [Ph₃C][B(C₆F₅)₄] activator did not have a significant effect on activity but did lower the molecular weight somewhat and broadened the molecular weight distribution ($M_w/M_n = 3.7$).

(ii) Ethylene Polymerization with 3a/MAO. The possibility of activating **3a** with methylalumoxane (MAO) was also briefly explored.³¹ Treatment of **3a** with MAO (Al/Zr = 1000/1) yields a very low activity catalyst (1.3 (kg of PE)(mol of cat)⁻¹ h⁻¹ atm⁻¹; at 30 °C, 8 atm). Furthermore, the polyethylene produced by the **3a**/MAO catalyst at 30 °C has a low molecular weight ($M_n = 13\,400$) and a very broad molecular weight distribution ($M_w/M_n = 28$). To probe the origin of the difference in behavior of the **3a**/B(C₆F₅)₃ and **3a**/MAO catalysts, the reactivity of **3a** with Al alkyls was investigated. ^1H NMR monitoring experiments establish that **3a** reacts rapidly with AlMe₃ to yield pyC(CF₃)₂OAlMe₂ as a principal product (ca. 50% of the pyC(CF₃)₂O containing products).³² This species is also produced by the reaction of alcohol **2a** with AlMe₃. Thus, the alkoxide ligands of **3a** are susceptible to abstraction by Al reagents, and complicated chemistry may be anticipated in the **3a**/MAO catalyst system. The broadening of the molecular weight distribution observed upon addition of Al(ⁱBu)₃ to the **3a**/[Ph₃C]-

[B(C₆F₅)₄] catalyst also may result from alkoxide transfer to Al.

(iii) Hexene Polymerization by 6a. Complex **6a** catalyzes the polymerization of 1-hexene to low molecular weight atactic polyhexene with moderate activity (90 (kg PH)(mol of cat)⁻¹ h⁻¹) under mild conditions (CD₂Cl₂, 23 °C). The ^1H NMR spectrum of the polyhexene produced by **6a** contains resonances for terminal (H₂C=CRR'; δ 4.72, 4.66) and internal (RHC=CR'H; δ 5.3) olefins in an intensity ratio of 7/4. These resonances correspond to end groups resulting from β -H elimination following 1,2 or 2,1 hexene insertions (eq 6). An M_n value of 840 (i.e., degree of polymerization



= 10) was determined by integration of these resonances versus the major 12H polyhexene resonance (δ 0.8–1.2). ^1H NMR monitoring of the hexene polymerization reveals rapid disappearance of the **6a** resonances and simultaneous appearance of polyhexene resonances.

Discussion

Dibenzyl complexes of the type (pyCR₂O)₂Zr(CH₂Ph)₂ (**3a–c**) adopt distorted octahedral structures with a *trans*-O, *cis*-N, *cis*-benzyl ligand arrangement. These complexes have idealized C₂ symmetry and are, thus, chiral; however, inversion of configuration at the metal is rapid on the NMR time scale at room temperature. The racemization barriers (from 8.6 (**3b**) to 10.1 (**3c**) kcal/mol) are significantly lower than those determined for the 8-quinolinolato systems (Ox)₂MR₂ (M = Zr, Hf; ΔG^\ddagger (racemization) = 15–18 kcal/mol). Ambient temperature NMR data reported by Holm for structurally analogous (pyCAr₂O)₂Mo(=O)₂ complexes establish that these systems are also configurationally labile, although racemization barriers were not determined.³ Some years ago Serpone showed that the closely related 8-quinolinolato phenoxide complex (Ox)₂Ti{O-2,6-(ⁱPr)₂-C₆H₃}₂, which adopts an analogous *trans*-O, *cis*-N, *cis*-phenoxide structure, undergoes racemization via a dissociative “bond rupture” mechanism.³³ Serpone proposed that racemization proceeds via a labile trigonal bipyramidal intermediate formed by Ti–N bond dissociation. It is likely that racemization of **3a–c** and (Ox)₂MR₂ complexes proceeds by the same mechanism. The lower barriers observed for **3a–c** reflect the fact that pyCR₂O⁻ ligands are more flexible than Ox⁻ ligands, which allows Zr–N bond dissociation without significant disruption of the Zr–O bond. Indeed, the pyridine ligands of **5d**, which albeit are *ortho*-disubstituted and thus very crowded, are easily displaced by THF. It is also possible, especially for the fluorinated system **3a**, that alkoxide dissociation leads to a labile intermediate and racemization. However, intermolecular exchange of the pyCH(CF₃)₂O⁻ ligands of **3c** occurs only slowly (hours) on the laboratory time scale.

(30) For use of CPh₃⁺ in the generation of Cp₂Zr(R)⁺ species, see: (a) Chien, J. C. W.; Tsai, W.; Rausch, M. D. *J. Am. Chem. Soc.* **1991**, *113*, 8570. (b) Ewen, J. A.; Elder, M. J. *Makromol. Chem., Macromol. Symp.* **1993**, *66*, 179. (c) Bochmann, M.; Lancaster, S. J. *Organometallics* **1993**, *12*, 633. (d) Razavi, A.; Thewalt, U. *J. Organomet. Chem.* **1993**, *445*, 111. See also (e) Straus, D. A.; Zhang, C.; Tilley, T. D. *J. Organomet. Chem.* **1989**, *369*, C13.

(31) For discussions of the use, possible structures, and possible mechanisms of the action of MAO, see (a) Sinn, H.; Kaminsky, W. *Adv. Organomet. Chem.* **1980**, *18*, 99. (b) Sishta, C.; Hathorn, R. M.; Marks, T. J. *J. Am. Chem. Soc.* **1992**, *114*, 1112. (c) Harlan, C. J.; Bott, S. G.; Barron, A. R. *J. Am. Chem. Soc.* **1995**, *117*, 6465.

(32) (a) ^1H NMR for pyC(CF₃)₂OAlMe₂ (CD₂Cl₂): δ 8.60 (d, $J = 5.3$ Hz, 1H, 6-py), 8.25 (td, $J = 7.9, 1.6$ Hz, 1H, 4-py), 8.03 (d, $J = 8.2$ Hz, 1H, 3-py), 7.86 (ddd, $J = 7.6, 5.5, 1.0$ Hz, 1H, 5-py), -0.67 (s, 6H). (b) A pentane solution (1 mL) of **2a** (30 mg, 0.12 mmol) was added to AlMe₃ (20 mg, 0.28 mmol) at 23 °C to give a white slurry. The volatiles were removed under vacuum to give a white solid, which dissolved in CD₂Cl₂ to give a clear colorless solution. The ^1H NMR spectrum revealed the presence of pyC(CF₃)₂OAlMe₂ (see ref 32a) and {pyC(CF₃)₂O}₂AlMe (ratio 8/2). ^1H NMR of {pyC(CF₃)₂O}₂AlMe (CD₂Cl₂): δ 8.76 (ddd, $J = 5.3, 1.6, 1.0$ Hz, 2H, 6-py), 8.13 (td, $J = 7.8, 1.8$ Hz, 2H, 4-py), 7.91 (d, $J = 8.3$ Hz, 2H, 3-py), 7.77 (ddd, $J = 6.4, 5.3, 1.1$ Hz, 2H, 5-py), -0.94 (s, 3H, Me). (c) Similar compounds have been described previously, see: van Vliet, M. R. P.; van Koten, G.; de Keijser, M. S.; Vrieze, K. *Organometallics* **1987**, *6*, 1652.

(33) Bickley, D. G.; Serpone, N. *Inorg. Chem.* **1979**, *18*, 2200.

Cationic five-coordinate species $(\text{pyCR}_2\text{O})_2\text{Zr}(\text{CH}_2\text{Ph})^+$ **6a–c** are generated from **3a–c** by alkyl abstraction or Zr–R protonolysis reactions. These species most likely adopt distorted square pyramidal structures (Chart 3) in which the ligand arrangement is strongly influenced by the π -donor properties of the alkoxide ligand. Cations **6a** and **6c** catalyze ethylene polymerization under mild conditions, while **6b**, which contains the relatively electron-donating pyCMe_2O^- ligand, does not. This trend is opposite to that reported for metallocene catalysts, in which incorporation of electron-donating substituents on the Cp ligands generally increases activity in the absence of overriding steric factors.³⁴ It is reasonable to assume that the active species in these polymerizations are $(\text{pyCR}_2\text{O})_2\text{Zr}(\text{P})^+$ cations (P = growing chains); however, at present, there is no definitive evidence on this point. The presence of benzyl end groups in, and the narrow molecular weight distribution of the polyethylene produced by **6a** indicate that polymerization is initiated by insertion into $\text{Zr–CH}_2\text{Ph}$ bonds and that the catalyst is a single site catalyst. Catalysts **6a** and **6c** exhibit much lower activity and produce much lower molecular weight polymers than metallocene catalysts under similar conditions (activity typically $>10^3$ (kg of PE)(mol of cat)⁻¹ h⁻¹ atm⁻¹).² The observed activity order **6a** > **6c** > **6b** suggests that these systems may be insufficiently electrophilic to efficiently bind and activate olefins for insertion.³⁵ This issue can be addressed in greater detail when more is known about the structures and reactivity of these cations.

This work provides an entry to neutral and cationic group 4 metal alkyl complexes based on octahedral geometries and tunable, bidentate pyridine–alkoxide ligands. The chemistry of related $(\text{pyCAr}_2\text{O})_2\text{MX}_2$ and $(\text{pyCAr}_2\text{O})_2\text{M}(\text{R})^+$ complexes, as well as strategies to increase the configurational stability and reactivity of these systems, will be described in later papers in this series.^{28,36}

Experimental Section

General Considerations. The following compounds were prepared by literature methods: 2-bromo-6-(trimethylsilyl)pyridine,³⁷ pyCHCF_3OH ,³⁸ $\text{Zr}(\text{CH}_2\text{Ph})_4$,³⁹ $\text{B}(\text{C}_6\text{F}_5)_3$,⁴⁰ and $[\text{HNMe}_2\text{Ph}][\text{B}(\text{C}_6\text{F}_5)_4]$.⁴¹ The lithium alkoxides were prepared with *n*-BuLi in hexane. NMR spectra were recorded on Bruker AMX-360 (¹H, ¹³C) or AC-300 (¹⁹F) instruments in flame-sealed or Teflon-valved tubes at 25 °C, unless otherwise indicated. ¹H and ¹³C chemical shifts are reported versus Me₄Si and were determined by reference to the residual solvent peaks. ¹³C NMR assignments and *J*_{CH} values are based on gated-¹H/¹³C spectra. The numbering system used for NMR assignments is given in Chart 2. Representative ligand syntheses and olefin polymerization experiments are described.

pyC(CF₃)₂OLi (1a). A hexane solution of *n*-BuLi (2.5 M, 3.9 mL, 9.8 mmol) was added dropwise at –78 °C over 25 min

to an Et₂O (20 mL) solution of $\text{pyC}(\text{CF}_3)_2\text{OH}$ (2.41 g, 9.84 mmol), affording a yellow slurry. The slurry was stirred at –78 °C for 2 h and allowed to warm to ambient temperature; the color changed to red. The volatiles were removed under vacuum, yielding a red solid. Benzene (20 mL) and then pentane (20 mL) were added, and the off-white solid was collected by filtration, washed with pentane (15 mL), and dried under vacuum. Yield: 1.7 g, 70%. ¹H NMR (C₆D₆): δ 8.41 (d, *J* = 4.2 Hz, 1H, 6-py), 7.54 (d, *J* = 8.1 Hz, 1H, 3-py), 6.82 (td, *J* = 8.0, 1.8 Hz, 1H, 4-py), 6.50 (ddd, *J* = 7.5, 5.0, 1.0 Hz, 1H, 5-py). ¹³C{¹H} NMR (C₆D₆): δ 156.7 (2-py), 148.9 (6-py), 137.1 (4-py), 125.6 (q, *J*_{CF} = 291 Hz, CF₃), 124.3 (5-py), 123.2 (3-py); the CF₃ and pyCO signals were not detected.

(6-SiMe₃)pyC(CF₃)₂OLi (1d). A hexane solution of *n*-BuLi (2.5 M, 6.8 mL, 17 mmol) was added dropwise at –25 °C over 1 h to an Et₂O solution (50 mL) of 2-bromo-6-(trimethylsilyl)pyridine (3.97 g, 16.5 mmol), and the yellow solution was stirred for 30 min. The temperature was increased to 4 °C, and the reaction mixture was stirred for 40 min, resulting a red solution. Hexafluoroacetone (17 mmol, 1.7 mL at –78 °C) was condensed in over 10 min at –78 °C. The color changed from red to yellow. The reaction mixture was allowed to warm to and maintained at ambient temperature for 15 h. The volatiles were removed at 60 °C under vacuum. The residue was extracted with Et₂O (30 mL), and the extract was concentrated to 15 mL. Pentane (10 mL) was added to afford a white slurry, which was cooled to –35 °C for 3 h. The white solid was collected by filtration and dried under vacuum. Yield 1.92 g, 36.0%. ¹H NMR (C₆D₆): δ 7.54 (d, *J* = 8.1 Hz, 2H, 3 or 5-py), 7.09 (dd, *J* = 7.5, 1.0 Hz, 2H, 3 or 5-py), 6.92 (t, *J* = 7.9 Hz, 2H, 4-py), 0.30 (s, 9H, CH₃). ¹³C{¹H} NMR (C₆D₆): δ 170.1 (6-py), 156.3 (2-py), 135.3 (4-py), 130.8 (5-py), 122.8 (3-py), –1.1 (SiMe₃); the CF₃ and COLi signals were not detected.

pyC(CF₃)₂OH (2a). A hexane solution of *n*-BuLi (2.5 M, 54.4 mL, 136 mmol) was added dropwise at –78 °C over 15 min to an Et₂O (200 mL) solution of 2-bromopyridine (13.0 mL, 136 mmol). The red solution was stirred for 10 min, and hexafluoroacetone (15 mL at –78 °C, ca. 150 mmol) was added over 1 h at –78 °C. The solution was allowed to warm to ambient temperature and stirred for 15 h. The reaction mixture was neutralized with aqueous [NH₄]Cl, and the organic layer was separated. The aqueous layer was extracted with ether (2 × 50 mL), and the combined ether fractions were dried over MgSO₄ and evaporated to afford a brown oil, which was vacuum distilled. The fraction boiling between 55 and 75 °C at 0.001 mmHg was collected (yellow oil, 3.2 g, 40%). ¹H NMR (C₆D₆): δ 7.81 (d, *J* = 4.0 Hz, 1H, 6-py), 7.50 (s, 1H, OH), 7.32 (d, *J* = 8.0 Hz, 1H, 3-py), 6.82 (m, 1H, 4-py), 6.3 (m, 1H, 5-py). ¹³C{¹H} NMR (CD₂Cl₂): δ 148.2 (6-py), 139.1 (4-py), 126.5 (5-py), 123.0 (br, 3-py), 122.9 (q, *J*_{CF} = 287 Hz, CF₃); the 2-py and pyCO signals were not detected.

pyCMe₂OH (2b). A hexane solution of *n*-BuLi (2.5 M, 42 mL, 105 mmol) was added dropwise at –78 °C over 20 min to an Et₂O (50 mL) solution of 2-bromopyridine, and the resulting red solution was stirred for 20 min. Acetone (7.7 mL, 105 mmol) was added via syringe over 20 min, and the dark green slurry was allowed to warm to room temperature and stirred for 12 h. Water (50 mL) was added, and the organic phase was separated. The aqueous phase was extracted with ether, and the combined ether fractions were dried over MgSO₄ and evaporated under vacuum to afford a brown oil. The oil was sublimed twice (50 °C, 0.005 mmHg) yielding a white solid (8.1 g, 56%). ¹H NMR (CDCl₃): δ 8.44 (d, *J* = 4.9 Hz, 1H, 6-py), 7.63 (td, *J* = 7.7, 1.7 Hz, 1H, 4-py), 7.32 (d, *J* = 8.0 Hz, 1H, 3-py), 7.12 (m, 1H, 5-py), 5.09 (s, 1H, OH), 1.48 (s, 6H, Me). ¹³C{¹H} NMR (CDCl₃): δ 165.9 (2-py), 147.3 (6-py), 136.8 (4-py), 121.7 (5-py), 118.6 (3-py), 71.6 (COH), 30.5 (Me).

(6-SiMe₃)pyC(CF₃)OH (2d). An Et₂O solution (50 mL) of (6-SiMe₃)pyC(CF₃)₂OLi (0.82 g) was washed with water (20 mL) four times. The Et₂O layer was dried over MgSO₄, which was filtered off. The volatiles were removed under vacuum, yielding a colorless oil. Yield: 0.71 g, 88%. ¹H NMR (C₆D₆):

(34) For example, see: Lee, I.-M.; Gauthier, W. J.; Ball, J. M.; Iyengar, B.; Collins, S. *Organometallics* **1992**, *11*, 2115.

(35) For a discussion of the d⁰ metal olefin complexes, see: Wu, Z.; Jordan, R. F.; Petersen, J. L. *J. Am. Chem. Soc.* **1995**, *117*, 5867.

(36) Kim, I.; Nishihara, Y.; Rogers, R. D.; Yap, G.; Rheingold, A. L.; Jordan, R. F. *Organometallics* **1997**, *16*, 3314.

(37) Jutzki, P.; Lorey, O. *J. Organomet. Chem.* **1976**, *104*, 153.

(38) Tordeaux, M.; Francese, C.; Wakselman, C. *J. Chem. Soc., Perkin Trans. 1* **1990**, 1951.

(39) Zucchini, U.; Albizzati, E.; Giannini, U. *J. Organomet. Chem.* **1971**, *26*, 357.

(40) Massey, A. G.; Park, A. J. *J. Organomet. Chem.* **1964**, *2*, 245.

(41) Tjaden, E. B.; Swenson, D. C.; Jordan, R. F. *Organometallics* **1995**, *14*, 371.

δ 8.03 (s, 1H, OH), 7.41 (dm, $J = 8$ Hz, 1H, 3-py), 7.06 (dd, $J = 7.4, 1.1$ Hz, 1H, 5-py), 6.98 (t, $J = 8.0$ Hz, 1H, 3-py), 0.06 (s, 9H, CH₃). ¹³C{¹H} NMR (CDCl₃): δ 167.2 (2-py), 145.7 (6-py), 136.3 (4- or 5-py), 130.8 (4- or 5-py), 122.4 (q, $J_{CF} = 287$ Hz, CF₃), 121.6 (3-py), -2.1 (CH₃); the pyCO signal was not detected. Anal. Calcd for C₁₁H₁₃F₆NOSi: C, 41.63; H, 4.14; N, 4.41. Found: C, 41.42; H, 4.12; N, 4.32

{pyC(CF₃)₂O}₂Zr(CH₂Ph)₂ (3a). A toluene solution (20 mL) of pyC(CF₃)₂OH (0.545 g, 2.16 mmol) was added to a toluene solution (20 mL) of Zr(CH₂Ph)₄ (0.492 g, 1.08 mmol) at 23 °C. The orange solution was stirred for 1 h at 23 °C and concentrated under vacuum until a precipitate appeared. Pentane (10 mL) was added, and the slurry was cooled to -35 °C. The orange solid was collected by filtration, washed with pentane, and dried under vacuum. Yield: 0.530 g, 65%. ¹H NMR (CD₂Cl₂): δ 7.92 (d, $J = 5.3$ Hz, 2H, 6-py), 7.86 (td, $J = 7.5, 1.6$ Hz, 2H, 4-py), 7.77 (d, $J = 8.1$ Hz, 2H, 3-py), 7.17 (ddd, $J = 7.4, 5.5, 1.2$ Hz, 2H, 5-py), 6.93 (t, $J = 7.7$ Hz, 4H, *m*-Ph), 6.77 (t, $J = 7.3$ Hz, 2H, *p*-Ph), 6.66 (d, $J = 7.2$ Hz, 4H, *o*-Ph), 2.07 (s, 4H, CH₂). ¹H NMR (-90 °C, CD₂Cl₂): δ 7.90 (d, $J = 4.8$ Hz, 2H, 6-py), 7.82 (t, $J = 7.8$ Hz, 2H, 4-py), 7.71 (d, $J = 7.8$ Hz, 2H, 3-py), 7.12 (t, $J = 6.3$ Hz, 2H, 5-py), 6.86 (br, 3H, *m*- and *p*-Ph), 6.42 (br, 2H, *o*-Ph), 1.65 (br s, 2H, CH₂), 1.24 (br s, 2H, CH₂). ¹³C{¹H} NMR (CD₂Cl₂): δ 154.3 (br, 2-py), 150.0 (6-py), 146.8 (*ipso*-Ph), 140.1 (4-py), 128.9 (*o*-Ph), 127.3 (*m*-Ph), 125.9 (5-py or *p*-Ph), 123.6 (q, $J_{CF} = 290$ Hz, CF₃), 123.1 (3-py), 121.8 (5-py or *p*-Ph), 89.1 (sept, $J_{CF} = 30$ Hz, pyCO), 68.3 ($J_{CH} = 125$ Hz, CH₂). ¹⁹F NMR (CD₂Cl₂): δ -78.0. Anal. Calcd for C₃₀H₂₂F₁₂N₂O₂Zr: C, 47.30; H, 2.92; N, 3.68. Found: C, 47.12; H, 2.77; N, 3.79.

{pyCMe₂O}₂Zr(CH₂Ph)₂ (3b). A toluene solution (5 mL) of pyCMe₂OH (284 mg, 2.07 mmol) was added to a toluene solution (10 mL) of Zr(CH₂Ph)₄ (472 mg, 1.04 mmol) at 23 °C. The orange solution was stirred for 2 h at 23 °C and concentrated under vacuum until a precipitate formed. Hexane (10 mL) was added, and the slurry was cooled to -35 °C. The orange powder was collected by filtration, washed with pentane, and dried under vacuum. Yield: 425 mg, 75%. Single crystals suitable for X-ray diffraction were obtained by crystallization at -35 °C from dichloromethane. ¹H NMR (CD₂Cl₂): δ 8.28 (d, $J = 5.3$ Hz, 2H, 6-py), 7.73 (t, $J = 7.1$ Hz, 2H, 4-py), 7.23 (d, $J = 8.0$ Hz, 2H, 3-py), 7.14 (t, $J = 6.7$ Hz, 2H, 5-py), 6.77 (t, $J = 7.5$ Hz, 4H, *m*-Ph), 6.50 (t, $J = 7.3$ Hz, 2H, *p*-Ph), 6.45 (d, $J = 7.4$ Hz, 4H, *o*-Ph), 2.05 (s, 4H, CH₂), 1.31 (s, 12H, CH₃). ¹H NMR (-100 °C, CD₂Cl₂): δ 8.42 (br s, 2H, 6-py), 7.74 (br t, 4-py), 7.19 (br d, $J = 5.3$ Hz, 3-py), 7.13 (t, $J = 7.5$ Hz, 5-py), 6.73 (br, 4H, *m*-Ph), 6.43 (br, 2H, *p*-Ph), 6.25 (br, 4H, *o*-Ph), 2.04 (br, 4H, CH₂), 1.81 (br, 2H, CH₂), 1.24 (br, 6H, CH₃), 0.95 (br, 6H, CH₃). ¹³C{¹H} NMR (CD₂Cl₂): δ 173.7 (2-py), 149.9 (*ipso*-Ph), 147.8 (6-py), 138.9 (4-py), 128.0 (*o*-Ph), 125.7 (*m*-Ph), 122.3, 121.0, 119.1 (3-py, 5-py, and *p*-Ph), 84.3 (COZr), 61.4 ($J_{CH} = 121$ Hz, CH₂), 31.65 (CH₃). Anal. Calcd for C₃₀H₃₄N₂O₂Zr: C, 66.00; H, 6.29; N, 5.13. Found: C, 65.84; H, 6.44; N, 5.21.

{pyCH(CF₃)O}₂Zr(CH₂Ph)₂ (3c). A benzene solution (30 mL) of pyCH(CF₃)OH (377 mg, 2.13 mmol) was added to a benzene solution (30 mL) of Zr(CH₂Ph)₄ (489 mg, 1.07 mmol) at 23 °C. The orange solution was stirred for 1 h at 23 °C. The volatiles were removed under vacuum. The yellow solid was slurried in a mixture of benzene (7 mL) and pentane (5 mL), collected by filtration, washed with pentane (15 mL), and dried under vacuum. Yield: 425 mg, 63%. This compound exists as a mixture of isomers as described in the text. ¹H NMR (CD₂Cl₂, (*R, R, \Lambda*) and (*R, R, \Delta*) isomers) at 23 °C, fast exchange): δ 8.00 (d, $J = 5.3$ Hz, 2H, 6-py), 7.68 (td, $J = 7.7, 1.6$ Hz, 2H, 4-py), 7.41 (d, $J = 8.0$ Hz, 2H, 3-py), 7.08 (t, $J = 6.5$ Hz, 2H, 5-py), 6.89 (t, $J = 7.5$ Hz, 4H, *m*-Ph), 6.67 (t, $J = 7.2$ Hz, 2H, *p*-Ph), 6.50 (d, $J = 7.2$ Hz, 4H, *o*-Ph), 5.52 (q, $J_{CF} = 7.4$ Hz, 2H, CHCF₃), 1.94 (d, $J = 8.6$ Hz, 1H, CH₂), 1.75 (d, $J = 8.6$ Hz, 1H, CH₂). ¹H NMR (CD₂Cl₂, (*R, R, \Lambda*) and (*R, R, \Delta*) isomers) at -90 °C, 3/1 isomer ratio, aliphatic region only): major isomer δ 5.68 (br q, $J = 6.5$ Hz, 2H, CHCF₃), 1.65 (br,

2H, CH₂), 0.83 (br, 2H, CH₂); minor isomer δ 4.95 (br, 2H, CHCF₃), 2.73 (br, 2H, CH₂), 2.01 (br, 2H, CH₂). ¹H NMR (CD₂Cl₂, (*R, S, \Lambda*) isomer) at 23 °C, rapid racemization): δ 8.14 (d, $J = 5.4$ Hz, 2H, 6-py), 7.70 (td, $J = 8.0, 1.6$ Hz, 2H, 4-py), 7.4 (3-py, partially obscured), 7.15 (t, $J = 6.6$ Hz, 2H, 5-py), 6.33 (d, $J = 7.3$ Hz, 2H, *o*-Ph), 5.47 (q, $J = 7.5$ Hz, 2H, CHCF₃), 2.20 (s, 2H, ZrCH₂), 1.46 (s, 2H, ZrCH₂), the other *o*-Ph signal and the *m*- and *p*-Ph signals obscured). ¹H NMR (CD₂Cl₂, (*R, S, \Lambda*) isomer) at -90 °C, slow racemization, aliphatic region only): δ 5.92 (q, $J = 5.8$ Hz, 1H, CHCF₃), 4.23 (q, $J = 7.7$ Hz, 1H, CHCF₃), 2.23 (d, $J = 6.8$ Hz, 1H, CH₂), 2.02 (br d, 1H, CH₂), 1.20 (d, $J = 7.9$ Hz, 1H, CH₂), -0.30 (d, $J = 8.6$ Hz, 1H, CH₂). ¹³C{¹H} NMR (CD₂Cl₂, rapidly exchanging (*R, R, \Lambda*) and (*R, R, \Delta*) isomers): δ 158.7 (2-py), 148.4 (6-py), 145.7 (*ipso*-Ph), 139.0 (4-py), 129.3 (*o*-Ph), 127.1 (*m*-Ph), 124.5 (5-py), 122.1 (q, $J_{CF} = 3$ Hz, 3-py), 121.4 (*p*-Ph), 81.8 (q, $J_{CF} = 31$ Hz, CHCF₃), 60.4 (CH₂, $J_{CH} = 130$ Hz). ¹³C{¹H} NMR (CD₂Cl₂, (*R, S, \Lambda*) isomer, rapid racemization): δ 158.5 (2-py), 148.2 (6-py), 147.0 and 144.4 (*ipso*-Ph), 138.9 (4-py), 130.0 and 128.4 (*o*-Ph), 127.7 and 126.6 (*m*-Ph), 124.6 (5-py), 122.3 and 120.4 (*p*-Ph), 121.9 (q, $J_{CF} = 3$ Hz, 3-py), 81.8 (q, $J_{CF} = 31$ Hz, CHCF₃), 62.4 (CH₂, $J_{CH} = 132$ Hz), 60.0 (CH₂, $J_{CH} = 127$ Hz).

{pyC(CF₃)₂O}₃ZrCl. Diethyl ether (30 mL) was added to a mixture of solid ZrCl₄ (116 mg, 0.500 mmol) and pyC(CF₃)₂OLi (374 mg, 1.49 mmol) at 23 °C. The white slurry was stirred for 18 h. The volatiles were removed under vacuum to afford a white solid, which was extracted with hot toluene (50 mL). The extract was concentrated under vacuum and cooled to -35 °C. The white solid was collected by filtration, washed with pentane, and dried under vacuum (338 mg, 79%). ¹H NMR (C₆D₆): δ 9.12 (d, $J = 5.3$ Hz, 3H, 6-py), 7.30 (d, $J = 8.0$ Hz, 3H, 3-py), 6.74 (td, $J = 7.7, 1.6$ Hz, 3H, 4-py), 6.54 (ddd, $J = 8.0, 5.6, 1.0$ Hz, 3H, 5-py). ¹³C{¹H} NMR (C₆D₆): δ 155.7 (2-py), 150.1 (6-py), 139.6 (4-py), 125.2 (5-py), 123.6 (q, $J_{CF} = 290$ Hz, CF₃), 122.8 (3-py); the COZr resonance was not detected. ¹⁹F NMR (C₆D₆): δ -74.6 (s, CF₃). Anal. Calcd for C₁₆H₁₂ClF₁₈N₃O₃Zr: C, 33.55; H, 1.41; N, 4.89; Cl, 4.13. Found: C, 33.37; H, 1.30; N, 4.92; Cl, 3.95.

{(6-SiMe₃)pyC(CF₃)₂O}₂ZrCl₂(THF)₂ (4d). Hexane (20 mL) was added to a mixture of solid ZrCl₄(THF)₂ (362 mg, 0.959 mmol) and (6-SiMe₃)pyC(CF₃)₂OLi (620 mg, 1.92 mmol), affording a white slurry, which was stirred for 18 h at 23 °C. The volatiles were removed under vacuum to afford a white solid, which was extracted with toluene (30 mL). The extract was cooled to -35 °C. The white solid was collected by filtration and dried under vacuum (604 mg, 59%). ¹H NMR (C₆D₆): δ 8.38 (d, $J = 7.7$ Hz, 2H, 3 or 5-py), 7.10 (t, $J = 7.4$ Hz, 2H, 4-py), 6.94 (d, $J = 7.4$ Hz, 2H, 3- or 5-py), 4.08 (br, 8H, THF), 1.20 (br, 8H, THF), 0.27 (s, 18H, SiMe₃).

{(6-SiMe₃)pyC(CF₃)₂O}₂ZrCl₂ (5d). A toluene solution (30 mL) of {(6-SiMe₃)pyC(CF₃)₂O}₂ZrCl₂(THF)₂ (315 mg, 0.295 mmol) was warmed at 95 °C under N₂ flow for 3 h. The volatiles were removed under vacuum to afford a colorless oil, which was dried under vacuum (65 °C, 17 h) to give a white solid. ¹H NMR (CD₂Cl₂): δ 8.02 (dd, $J = 7.7, 1.1$ Hz, 2H, 3- or 5-py), 7.94 (t, $J = 7.9$ Hz, 2H, 4-py), 7.67 (d, $J = 8.0$ Hz, 2H, 3- or 5-py), 0.64 (s, 18H, CH₃). ¹³C{¹H} NMR (CD₂Cl₂): δ 172.5 (6-py), 155.1 (2-py), 137.8 (4-py), 134.9 (5-py), 123.1 (3-py), 122.6 (q, $J_{CF} = 290$ Hz, CF₃), 76.3 (COZr), 1.8 (SiMe₃). ¹⁹F NMR (CD₂Cl₂): δ -74.4 (s, CF₃). Anal. Calcd for C₂₂H₂₄Cl₂F₁₂N₂O₂Si₂Zr: C, 33.24; H, 3.05; N, 3.53. Found: C, 33.50; H, 2.97; N, 3.38.

{[pyC(CF₃)₂O]₂Zr(CH₂Ph)][PhCH₂B(C₆F₅)₃] (6a). A benzene solution (3 mL) of B(C₆F₅)₃ (68.6 mg, 0.134 mmol) was added to a benzene solution (5 mL) of {pyC(CF₃)₂O}₂Zr(CH₂Ph)₂ (102.6 mg, 0.135 mmol) at 23 °C. A yellow oil separated. The mixture was stirred for 25 min at 23 °C. The volatiles were removed under vacuum. The yellow solid was washed with pentane and dried under vacuum to afford a yellow solid (97 mg, 57%). ¹H NMR (CD₂Cl₂): δ 8.33 (m, 4H, 4- and 6-py), 7.98 (d, $J = 8$ Hz, 2H, 3-py), 7.87 (t, $J = 6.5$ Hz, 2H, 5-py), 7.57 (br, 2H, *meta*-ZrCH₂Ph), 7.28 (t, $J = 7.4$ Hz, 1H, *para*-

ZrCH₂Ph), 7.00 (d, $J = 7.3$ Hz, 2H, *ortho*-ZrCH₂Ph), 6.88 (t, $J = 7$ Hz, 2H, *meta*-BCH₂Ph), 6.79 (t, $J = 6.6$ Hz, 1H, *para*-BCH₂Ph), 6.76 (d, $J = 7.3$ Hz, 2H, *ortho*-BCH₂Ph), 3.42 (s, 2H, ZrCH₂), 2.82 (s, 2H, BCH₂). ¹H NMR (−80 °C, CD₂Cl₂): δ 8.84 (d, $J = 4.8$ Hz, 1H, 6-py), 8.35 (t, $J = 7.7$ Hz, 1H), 8.13 (t, 1H), 8.04 (d, $J = 7.4$ Hz, 1H, 3-py), 7.95 (t, $J = 6.3$ Hz, 1H), 7.86 (t, 7.1 Hz, 1H), 7.73 (m, 3H), 7.63 (d, $J = 5.0$ Hz, 1H, 6-py), 7.02 (d, 1H, *ortho*-ZrCH₂Ph), 6.8 (m, 3H, *meta*- and *para*-BCH₂Ph, *ortho*-ZrCH₂Ph), 6.61 (d, $J = 7.0$ Hz, 2H, *ortho*-BCH₂Ph), 3.49 (d, $J = 8.2$ Hz, 1H, ZrCH₂Ph), 3.20 (d, $J = 8.3$ Hz, 1H, ZrCH₂-Ph), 2.68 (s, 2H, BCH₂Ph); the *para*-ZrCH₂Ph signal and one *meta*-ZrCH₂Ph signal are obscured. ¹⁹F NMR (CD₂Cl₂): δ −76.2 (12F, CF₃), −131.3 (d, $J_{\text{FF}} = 21.5$ Hz, 6F, *o*-C₆F₅), −164.9 (t, $J_{\text{FF}} = 20.5$ Hz, 3F, *p*-C₆F₅), −167.8 (t, $J_{\text{FF}} = 18.9$ Hz, 6F, *m*-C₆F₅). ¹³C NMR (CD₂Cl₂): δ 78.9 (ZrCH₂, $J_{\text{CH}} = 142$ Hz), 32 (br, BCH₂). Anal. Calcd for C₄₈H₂₂BF₂₇N₂O₂Zr: C, 45.26; H, 1.74; N, 2.20. Found: C, 43.80; H, 2.03; N, 2.33. The low C analysis may reflect thermal decomposition.

Generation of [(pyC(CF₃)₂O)₂Zr(CH₂Ph)] [B(C₆F₅)₄] (7a). Benzene (0.5 mL) was added to a mixture of {pyC(CF₃)₂O}₂-Zr(CH₂Ph)₂ (23.5 mg, 0.031 mmol) and [HNMe₂Ph][B(C₆F₅)₄] (25.2 mg, 0.031 mmol). A brown oil separated. The mixture was shaken for 20 min at 23 °C. Pentane was added, and the benzene/pentane layer was decanted. The yellow oil was washed with pentane and dried under vacuum, yielding a yellow solid. ¹H NMR (CD₂Cl₂): δ 8.33 (m, 4H, 4- and 6-py), 8.00 (d, $J = 8$ Hz, 2H, 3-py), 7.91 (t, 2H, $J = 6.7$ Hz, 5-py), 7.5 (br, 2H, *m*-Ph), 7.30 (t, $J = 7.6$ Hz, *p*-Ph), 7.02 (d, $J = 7.5$ Hz, *o*-Ph), 3.43 (s, 2H, ZrCH₂Ph).

[(pyCMe₂O)₂Zr(CH₂Ph)] [PhCH₂B(C₆F₅)₃] (6b). A benzene solution (10 mL) of B(C₆F₅)₃ (116 mg, 0.227 mmol) was added dropwise to a benzene solution (20 mL) of (pyCMe₂O)₂-Zr(CH₂Ph)₂ (124 mg, 0.228 mmol) over 10 min. A yellow oil separated, and the mixture was stirred for 1.5 h at 23 °C. The benzene layer was decanted, and the oil was washed with benzene (2 × 10 mL) and dried under vacuum to afford a yellow solid. Yield: 153 mg, 64%. The ¹H NMR spectrum established that this compound exists of two isomers (3/2 ratio). ¹H NMR (CD₂Cl₂, aliphatic region only): major isomer δ 3.15 (d, $J = 10.7$ Hz, 1H, CH₂), 2.90 (d, $J = 10.7$ Hz, 1H, CH₂), 2.80 (s, 2H, BCH₂Ph), 2.13 (s, 3H, CH₃), 1.69 (s, 3H, CH₃), 1.61 (s, 3H, CH₃), 1.40 (s, 3H, CH₃); minor isomer δ 2.82 (d, partially obscured, CH₂), 2.80 (s, 2H, BCH₂Ph), 2.67 (d, $J = 11.2$ Hz, 1H, CH₂), 2.31 (s, 3H, CH₃), 1.86 (s, 3H, CH₃), 1.81 (s, 3H, CH₃), 1.58 (s, 3H, CH₃); the aromatic region is complex. ¹³C NMR (CD₂Cl₂, both isomers): δ 173.5 (2-py, major), 173.2 (2-py, minor), 165.1 (2-py, major), 163.9 (2-py, minor), 148.9, 148.6 (dm, $J_{\text{CF}} = 234$ Hz, C₆F₅), 147.7, 146.1, 146.0, 145.0, 143.5, 143.3, 143.2, 142.3, 140.9, 137.8 (dm, $J_{\text{CF}} = 244$ Hz, C₆F₅), 136.7 (dm, $J_{\text{CF}} = 254$ Hz, C₆F₅), 130.2, 129.5, 129.2, 129.0, 128.7, 128.4, 128.2, 127.1, 126.8, 125.5, 125.2, 125.2, 125.1, 123.5, 123.3, 122.8, 122.6, 122.2, 90.7 (CO, major), 90.5 (CO, minor), 90.0 (CO, minor), 89.2 (CO, major), 77.1 (minor ZrCH₂, $J_{\text{CH}} = 119$ Hz), 75.3 (major ZrCH₂, $J_{\text{CH}} = 126$ Hz), 34.0 (Me, minor), 32.7 (2Me, major), 32.1 (Me, minor), 31.7 (Me and BCH₂ minor), 31.3 (Me, major), 31.1 (Me, minor), 30.5 (Me, major).

Generation of [(pyCMe₂O)₂Zr(CH₂Ph)] [B(C₆F₅)₄] (7b). Benzene (0.5 mL) was added to a mixture of (pyCMe₂O)₂-Zr(CH₂Ph)₂ (18.4 mg, 0.034 mmol) and [HNMe₂Ph][B(C₆F₅)₄] (27.3 mg, 0.034 mmol). A yellow oil separated. The mixture was shaken for 15 min at 23 °C. The benzene layer was decanted, and the oil was washed with benzene (3 × 0.5 mL). The oil was dried under vacuum to afford a yellow solid. The ¹H NMR spectrum established that this compound consists of

two isomers (3/2 ratio). ¹H NMR (CD₂Cl₂, aliphatic region only): major isomer δ 3.18 (d, $J = 10.5$ Hz, 1H, CH₂), 2.93 (d, $J = 10.7$ Hz, 1H, CH₂), 2.16 (s, 3H, Me), 1.71 (s, 3H, Me), 1.63 (s, 3H, Me), 1.43 (s, 3H, Me); minor isomer δ 2.88 (d, $J = 11$ Hz, 1H, CH₂), 2.68 (d, $J = 11$ Hz, 1H, CH₂), 2.35 (s, 3H, Me), 1.88 (s, 3H, Me), 1.83 (s, 3H, Me), 1.63 (s, 3H, Me).

Ethylene Polymerization with 6a from 3a and B(C₆F₅)₃. The following procedure is representative. Benzene (30 mL) was added to a mixture of **3a** (14 mg, 0.018 mmol) and B(C₆F₅)₃ (9.1 mg, 0.018 mmol) in a Fischer–Porter bottle at 23 °C under N₂. The yellow solution was stirred for 10 min. The N₂ was replaced by ethylene (3.3 atm), and polymerization was carried out for 30 min at 40 °C. Polyethylene precipitated immediately. Methanol (80 mL) was added to quench the polymerization, and the polymer was collected by filtration and dried under vacuum. Polymer yield 0.96 g; activity 32 (kg of PE)(mol of cat)^{−1} atm^{−1} h^{−1}. Polymer analysis: $M_n = 6,200$, $M_w/M_n = 2.6$, $T_m = 128$ °C (DSC), 1 vinyl group/chain by ¹H NMR, PhCH₂ end group by ¹H NMR (25% of amount predicted assuming all **3a** is activated), 0.6 branches (>C₅)/chain by ¹³C NMR.

Ethylene Polymerization with 7a from 3a and [Ph₃C][B(C₆F₅)₄]. Conditions: 1 L autoclave, 500 mL of toluene, 44 μmol of **3a**, 44 μmol of [Ph₃C][B(C₆F₅)₄], 45 °C, 8 atm, 60 min. Activity: 56 (kg of PE)(mol of cat)^{−1} h^{−1} atm^{−1}. $M_n = 10,400$, $M_w/M_n = 2.8$. With added Al(^{*i*}Bu)₃ (17 equiv vs **3a**), activity = 60 (kg of PE)(mol of cat)^{−1} h^{−1} atm^{−1}, $M_n = 5,900$, $M_w/M_n = 3.7$.

Ethylene Polymerization with 7a from 3a and [HNMe₂Ph][B(C₆F₅)₄]. Conditions: Fischer–Porter bottle, 30 mL of benzene, 20 μmol of **3a**, 19 μmol of [HNMe₂Ph][B(C₆F₅)₄], 42 °C, 3.3 atm, 30 min. Yield 0.42 g; activity 13 (kg of PE)(mol of cat)^{−1} atm^{−1} h^{−1}.

Ethylene Polymerization with 3c/B(C₆F₅)₃. Conditions: Fischer–Porter bottle, 30 mL of toluene, 16 μmol of **3c**, 16 μmol of B(C₆F₅)₃, 40 °C, 3.3 atm, 30 min. Yield 0.074 g; activity 2.6 (kg of PE)(mol of cat)^{−1} atm^{−1} h^{−1}.

Ethylene Polymerization with 3a and MAO. Conditions: 1 L autoclave, 500 mL of toluene, 44 μmol of **3a**, 44 mmol of MAO (per Al basis), 45 °C, 8 atm, 60 min. Yield 0.46 g; activity: 1.3 (kg of PE)(mol of cat)^{−1} h^{−1} atm^{−1}. $M_n = 13,000$; $M_w/M_n = 28.2$.

Hexene Polymerization with 6a. Compound **6a** (32 mg, 0.025 mmol) was dissolved in CD₂Cl₂ (0.5 mL) to give a yellow solution. 1-Hexene (4.6 mmol) was added via vacuum transfer at −78 °C, and the solution was warmed to 23 °C for 10 min. ¹H NMR analysis of the reaction mixture showed that the 1-hexene was 98% converted to polyhexene, corresponding to an activity of 90 (kg PH)(mol of cat)^{−1} h^{−1}. The volatiles were removed yielding a sticky solid, which was washed with methanol and dried under vacuum. $M_n = 840$ by ¹H NMR; microstructure atactic by ¹³C NMR.⁴²

Acknowledgment. This work was supported by DOE Grant No. DE-FG02-88ER13935 and the Mitsubishi Chemical Corporation.

Supporting Information Available: Tables giving crystallographic data, positional and thermal parameters, and bond distances and angles for **3b** (11 pages). Ordering information is given on any current masthead page.

OM9702439

(42) (a) Babu, G. N.; Newmark, R. A.; Chien, J. C. W. *Macromolecules* **1994**, *27*, 3383. (b) Asakura, T.; Demura, M.; Nishiyama, Y. *Macromolecules* **1991**, *24*, 2334.